



Project No: 603502

DACCIWA

"Dynamics-aerosol-chemistry-cloud interactions in West Africa"

Deliverable

D3.4 Present emissions

<u>Due date of deliverable:</u>	31/05/2018		
<u>Completion date of deliverable:</u>	04/06/2018		
Start date of DACCIWA project:	1 st December 2013	Project duration:	60 months
Version:	[V1.0]		
File name:	[D3.4_Present_emissions_DACCIWA_v1.0.pdf]		
Work Package Number:	3		
Task Number:	4		
<u>Responsible partner for deliverable:</u>	UoY		
Contributing partners:	KIT, ETHZ, UPMC, ECMWF		
Project coordinator name:	Prof. Dr. Peter Knippertz		
Project coordinator organisation name:	Karlsruher Institut für Technologie		

The DACCIWA Project is funded by the European Union's Seventh Framework Programme for research, technological development and demonstration under grant agreement no 603502.

Dissemination level		
PU	Public	x
PP	Restricted to other programme participants (including the Commission Services)	
RE	Restricted to a group specified by the consortium (including the Commission Services)	
CO	Confidential, only for members of the consortium (including the Commission Services)	

Nature of Deliverable		
R	Report	x
P	Prototype	
D	Demonstrator	
O	Other	

Copyright

This Document has been created within the FP7 project DACCIWA. The utilization and release of this document is subject to the conditions of the contract within the 7th EU Framework Programme. Project reference is FP7-ENV-2013-603502.

DOCUMENT INFO**Authors**

Author	Beneficiary Short Name	E-Mail
Mat Evans	UoY	mat.evans@york.ac.uk
Eleanor Morris	UoY	erm552@york.ac.uk
Tanja Stanelle	ETHZ	tanja.stanelle@env.ethz.ch
Federica Pacifico	UPS	federica.pacifico@gmail.com
Claire Delon	UPS	claire.delon@aero.obs-mip.fr
Pamela Dominutti	UBP	p.dominutti@opgc.univ-bpclermont.fr
Agnès Borbon	UBP	a.borbon@opgc.univ-bpclermont.fr
Adrien Deroubaix	UPMC	adrien.deroubaix@lmd.polytechnique.fr
Laurent Menut	UPMC	menut@lmd.polytechnique.fr
Cyrille Flamant	UPMC	cyrille.flamant@latmos.ipsl.fr

Changes with respect to the DoW

Issue	Comments
None	None

Dissemination and uptake

Target group addressed	Project internal / external

Document Control

Document version #	Date	Changes Made/Comments
V0.1	23.03.2018	Template with basic structure
V0.1	13.05.2018	Initial draft produced by Mat Evans. Circulated to the authors
V0.3	19.05.2018	Draft circulated to the authors.
V0.4	23.05.2018	Draft circulated to the WP.
V0.5	25.05.2018	Placed on Sharepoint for approval of the general assembly
V1.0	04.06.2018	Final document approved by the general assembly

Table of Contents

1 Foreword	5
2 Summary	6
3 Models used for the evaluations	8
3.1 GEOS-Chem (UoY)	8
3.2 CHIMERE (UPMC)	10
3.3 ECHAM6-HAM2 (ETHZ)	10
4 Natural Emissions	11
4.1 Isoprene (UoY)	11
4.2 Soil NO _x (UPS)	13
5 Evaluation of biomass burning emissions	14
5.1 CHIMERE (UPMC)	15
5.2 GEOS-Chem (UoY)	16
6 Evaluation of anthropogenic emissions	18
6.1 CHIMERE (UPMC)	18
6.2 GEOS-Chem (UoY)	21
6.3 ECHAM6-HAM2 (ETHZ)	25
6.4. VOC emissions from cities (UBP)	31
7 Impacts of emissions on policy relevant species during the DACCIWA campaign period	32
7.1 Impact of biomass burning (UoY)	32
7.2 Impacts of anthropogenic emissions (UoY)	33
8 DACCIWA Developed Emissions Inventories	35
8.1 Anthropogenic Emissions	35
8.2 Oil Flaring	36
9.0 Conclusions	37

1 Foreword

This report outlines the conclusions of research undertaken as part of the DACCIWA project as to our understanding of present day emissions of air pollutants and their precursors over southern West Africa, and their impact on the composition of the atmosphere in the region. The content is composed of various studies undertaken by DACCIWA partners (UoY, UPS, UPB, UPMC, ETHZ). Some of this material has already been published or is awaiting publication. Where the publications are available they are referenced and included in the bibliography at the end of the document.

2 Summary

This report focuses on the emissions of compounds into the air above southern West Africa during the summer months of the DACCIWA aircraft campaign (*Knippertz et al., 2017; Flamant et al., 2018*). During this period the meteorological conditions reduce the importance of sources which dominate in the winter months (desert dust from the Sahara and local biomass burning) and which may dominate in the annual average. Thus we focus on natural (isoprene, soil NO_x), remote biomass burning (predominantly from central Africa) and regional anthropogenic emissions. A collection of different studies from the DACCIWA partners have evaluated a variety of these emissions. These evaluations have taken many forms including comparing the predictions of chemistry transport models against observations, the direct measurement of fluxes, or the evaluation of individual emissions sources.

The natural emissions (isoprene and soil NO_x) appear to be simulated relatively well by the available models, especially given known spatial and temporal variability (see Section 4.1). Their importance compared to the anthropogenic source significantly larger in this region than in other regions such as Europe and North America. Thus ensuring that these emissions are correctly quantified and parameterized for air quality models, and how they change over the next decades, will be an important area of research to correctly assess the future composition of the atmosphere in the region.

Biomass burning in central Africa is a large source of pollutants into the region. Evaluating their emissions 2,000 km from their source is difficult but it appears that the current GFAS emissions from ECMWF are not inconsistent with the observations from DACCIWA. Increasing emissions by a factor of 3.4 (as suggested by *Kaiser et al., 2012*) appears to give improved results for organic carbon but would increase CO and black carbon concentrations beyond what was observed during DACCIWA.

Measurement of emissions from motor vehicles suggests a substantial (50 fold) missing source of some volatile organic compounds in the current generation of anthropogenic emissions inventories.

EDGAR (*EC-JRC/PBL, 2011*) is the current standard anthropogenic emissions inventory used by research and operational groups (ECMWF CAMS, NASA GEOS). A comparison between those emissions and the DACCIWA developed emissions inventory (*Junker et al., 2008; <http://eccad.aeris-data.fr>*) (Table 1) shows substantial differences in southern West Africa. NO_x emissions are a factor of 2.5 higher in the DACCIWA emissions, CO emissions are 56% higher, SO₂ emissions are 46% lower etc. than those in the EDGAR emissions.

Comparisons of the DACCIWA emissions to the DACCIWA observations show that CO, black carbon and organic carbon appear relatively well simulated. However, NO_x shows underestimates by factors from 50%-300% and SO₂ shows underestimates by a factor of 1,000%. Comparisons with the EDGAR emissions are generally less good and would require large changes to fit the observations.

The underestimates found in the anthropogenic emissions inventories appear to have a modest impact in the summer time O₃ calculated in the southern West African cities. But it has a significant impact on the PM_{2.5} calculated which is underestimated by a factor of 4 in the EDGAR emissions compared to those using the DACCIWA emissions scaled to the observations.

In general it would appear that the current generation of emissions inventories for West Africa substantially underestimate the emissions of virtually all pollutants and precursors. Air quality

forecasts for the region and estimates of human health and ecosystem impacts likely therefore underestimate the concentration of pollutants.

3 Models used for the evaluations

A number of models have been used for these evaluations. A brief description of the models and the configurations used for these studies are described below.

3.1 GEOS-Chem (UoY)

GEOS-Chem is a global and regional offline chemistry transport model (www.geos-chem.org; *Bey et al., 2001*). In this work we have run the model in its global configuration with $2^\circ \times 2.5^\circ$ horizontal resolution, and used this to provide a one way nesting with a regional grid run at $0.25^\circ \times 0.3125^\circ$ horizontal resolution over West Africa. See Figure 1.

We have used GEOS-Chem v11-01 which contains a O_x , HO_x , NO_x , VOC, BrO_x chemistry scheme and a mass based aerosol module which advects SO_4^{2-} , NO_3^- , NH_4^+ , Sea Salt, Dust, Organic and Black Carbon aerosol.

Emissions within the DACCIIWA region are described in Table 1. We have run simulations with both EDGAR (*EC-JRC/PBL, 2011*) and DACCIIWA (*Junker et al., 2008*) anthropogenic emissions. Biogenic emission use the MEGAN inventory (*Guenther et al., 2012*). Biomass burning uses GFAS emissions from ECMWF (*Kaiser et al., 2009*). Dust follows the work of *Zender et al. (2003 a,b)*, sea-salt of *Alexander et al. (2005)* and *Jaeglé et al. (2011)*, marine emissions of DMS are from *Breider et al. (2017)*, biogenic soil NO_x emissions from *Hudman et al. (2012)* and lightning NO_x is described by *Murray et al. (2012)*.

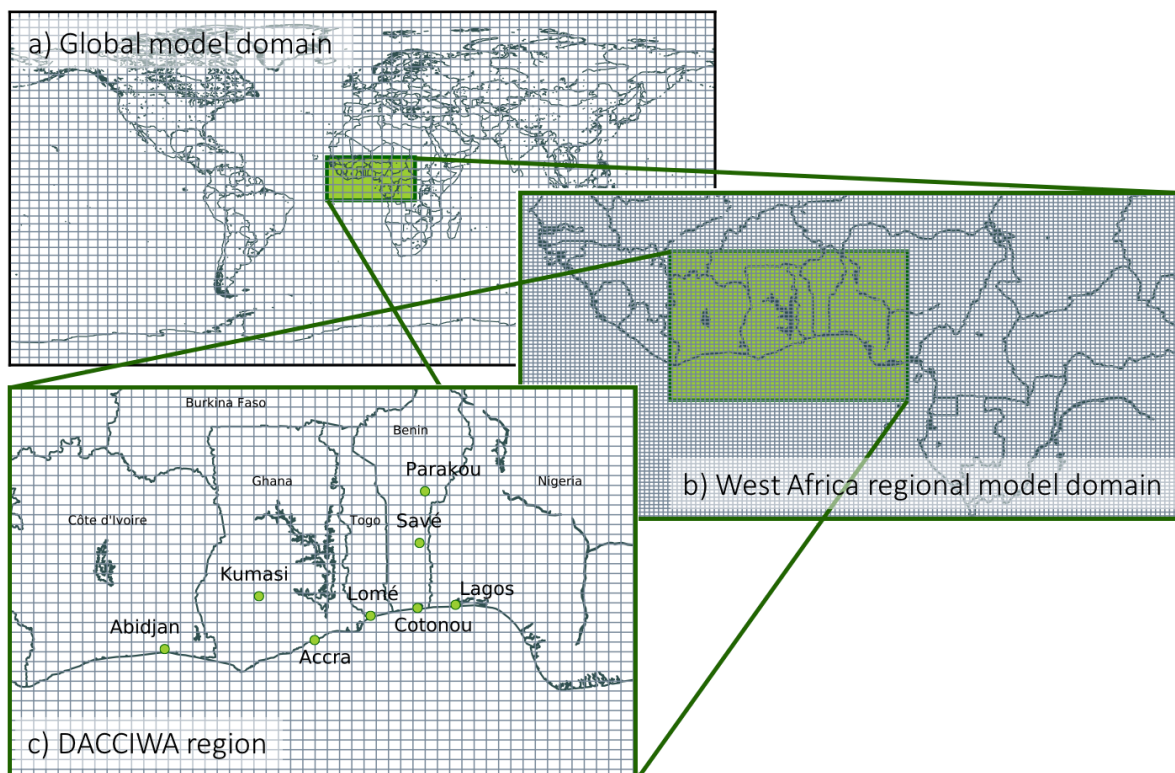


Figure 1. Global and regional GEOS-Chem grids used in the modelling work described here. a) shows the global domain; b) shows the regional domain run at $0.25^\circ \times 0.3125^\circ$ covering West Africa from the Atlantic coast to central Africa; c) shows the DACCIIWA operational area with the grid spacing used.

Species	Emission Type	Mean Daily Emission During Campaign / Gg day ⁻¹	Annual Emission / Gg yr ⁻¹
NO	Soil (Hudman et al.)	5.1	1859
	Biomass Burning (GFAS)	2.4	870
	Anthropogenic (EDGAR)	1.5	550
	Anthropogenic (DACCIWA)	3.6	1319
CO	Biomass Burning (GFAS)	77	28249
	Anthropogenic (EDGAR)	65	23661
	Anthropogenic (DACCIWA)	101	36893
SO ₂	Biomass Burning (GFAS)	0.49	179
	Anthropogenic (EDGAR)	1.08	394
	Anthropogenic (DACCIWA)	0.58	213
OC	Biomass Burning (GFAS)	3.8	1399
	Anthropogenic (EDGAR)	0.12	45
	Anthropogenic (DACCIWA)	8.5	3086
BC	Biomass Burning (GFAS)	0.54	196
	Anthropogenic (EDGAR)	0.06	24
	Anthropogenic (DACCIWA)	1.18	429
DMS	Ocean (Breider et al.)	1.33	484
NH ₃	Natural (GEIA)	40	14755
	Biomass Burning (GFAS)	0.86	316
	Anthropogenic (EDGAR)	2.4	879
VOCs	Biogenic (MEGAN)	151	55258
	Biomass Burning (GFAS)	6.3	2305
	Anthropogenic (EDGAR)	3.3	1214
	Anthropogenic (DACCIWA)	11	4064

Table 1. Average emissions during the DACCIWA period (29th June - 16th July 2016) within the West Africa region in the GEOS-Chem model (see Figure 1b). Emissions are given as a daily average during the aircraft campaign period, and as an annual value calculated using the average campaign data.

The GEOS-Chem model has been run in its regional West African configuration for the duration of the DACCIWA aircraft campaign following the tracks of the three aircrafts (see Figure 2) (*Flamant et al., 2017*) outputting the concentrations of all measured compounds and key fluxes.

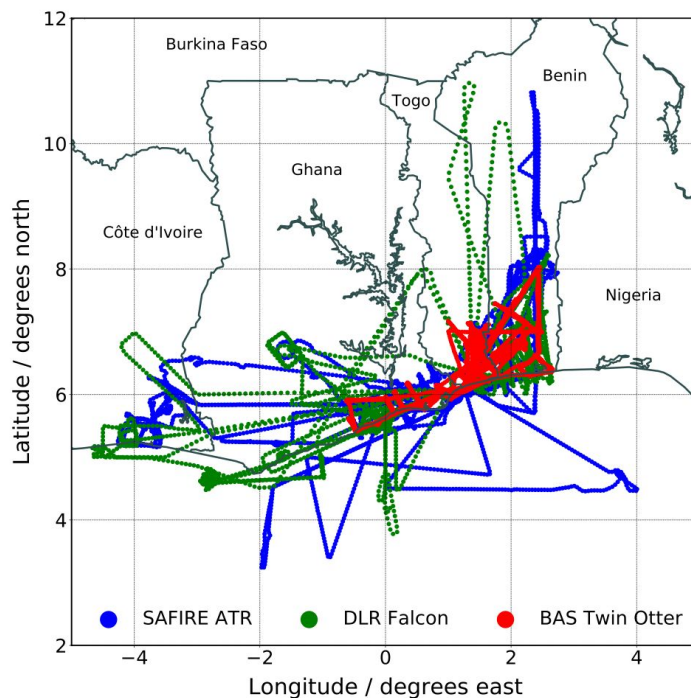


Figure 2. Flight tracks taken by the three research aircraft during the DACCIWA campaign from 29th June to 16th July 2016.

3.2 CHIMERE (UPMC)

CHIMERE is a chemistry-transport model allowing the simulation of concentration fields of gaseous and aerosols species at a regional scale. It is an off-line model version, driven by pre-calculated meteorological fields. In this study, the version is fully described in *Menut et al. (2013)* and updated in *Mailler et al. (2017)*. The simulations are performed with the same horizontal domain, the 28 vertical levels of the WRF simulations are projected onto 20 levels from the surface up to 200 hPa for CHIMERE.

Two simulations have been done with two different meteorological fields and resolutions (0.3° and 0.1°). The highest resolution has been nested with the lowest resolution for aerosol and gas concentrations. The meteorological fields used are ECMWF (for the 0.3° resolution) and WRF (for the 0.1° resolution).

3.3 ECHAM6-HAM2 (ETHZ)

The ECHAM6-HAM2 model is a global aerosol climate model. ECHAM6 is the sixth generation of the atmospheric general circulation model ECHAM. It is described in detail in *Stevens et al. (2013)*. The aerosol module HAM was first implemented in the 5th generation of ECHAM (*ECHAM5; Roeckner et al., 2003*) by the Max Planck Institute for Meteorology (*Stier et al., 2005*). Over the past years, the HAM module has been improved and completed with new processes (HAM2) as described in *Zhang et al. (2012)*. The HAM2 module is now coupled to the ECHAM6.

Aerosol microphysics is simulated using the M7 module (*Vignati et al., 2004*), which accounts for sulfate, black carbon, particulate organic matter, sea salt and dust. The atmospheric aerosol population is described as a superposition of seven lognormal distributed modes for which standard deviations are prescribed. The total number concentration and masses of the different chemical components are prognostic variables in the model. The modes are divided into soluble, internally mixed modes (containing sulfate) and insoluble, externally mixed modes which are

assigned to different size ranges. The modal diameters can vary and are calculated at each time step from the mass and number concentrations for each mode. Dust particles are considered as part of the soluble and insoluble accumulation and coarse modes. Sedimentation and dry and wet deposition are parameterized as functions of the aerosol size distribution, composition, and mixing state and depend on the ECHAM6 meteorology. The emission fluxes of dust, sea salt, and dimethyl sulfide from the oceans (DMS) are calculated online, based on the model meteorology. Anthropogenic emissions are prescribed. For more details see *Lohmann et al. (1996)* and *Lohmann et al. (2007)*.

For the DACCIWA project we choose to perform model simulations with the recent developed model version ECHAM6.3-HAM2.3. We performed simulations in T63L47 resolution (approx. 200 km x 200 km horizontal resolution). In the following we will base our analysis on simulations performed in free mode, which means that the large-scale circulation is not prescribed. The model is able to account for feedbacks between aerosols and the atmosphere (via the direct and indirect aerosol effect). But the sea surface temperature (SST) and the sea ice cover (SIC) are prescribed by AMIP data (<https://pcmdi.llnl.gov/mips/amip/amip2/>). Therefore, the SST and SIC are not able to adjust to changes in the atmosphere. The performed simulations differ in the applied emission inventory, they are summarized in Table 4. Emission fluxes of the year 2010 are read in for the entire simulation period. The simulation is assumed to represent the current climate, the simulation period covers 14 years (excluding 1 year spin up), here we present temporal averages over the simulation period.

4 Natural Emissions

Natural emissions play an important role in determining the chemical composition over southern West Africa. Table 1 shows the natural emissions of isoprene and soil NO_x calculated by the GEOS-Chem model. It is evident that the isoprene from vegetation dominates the regional anthropogenic VOC emissions and that soil NO_x plays an important role with emissions 36% higher than those from the DACCIWA anthropogenic emissions and ~220% higher than those from EDGAR. Thus, these emission types likely play a more significant role in southern West Africa than in other regions (Europe, North America). Over a year, emissions of dust from the Sahara to the north and local biomass burning play a significant role in determining the local pollution. But during the summer, when the DACCIWA aircraft campaign occurred, the monsoonal meteorology makes these sources much less significant.

4.1 Isoprene (UoY)

Figure 3 shows the distribution of isoprene emissions calculated in the GEOS-Chem model. The distribution follows the location of forested areas in the region.

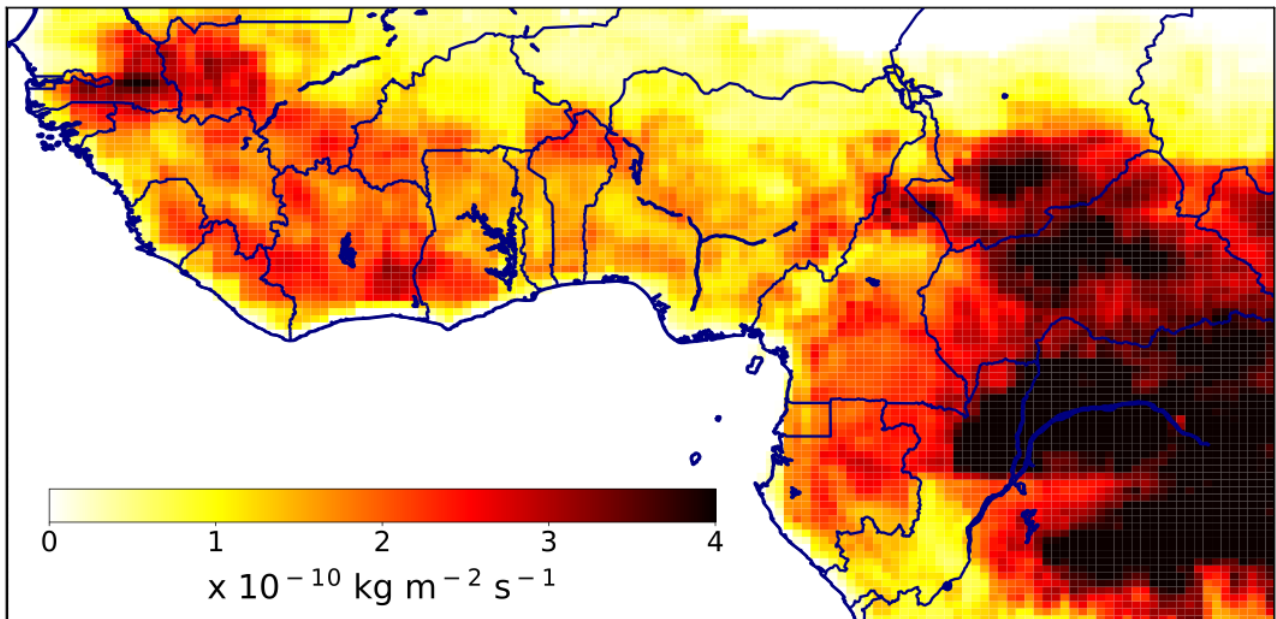


Figure 3. Isoprene emissions over southern Western Africa averaged for the DACCIWA campaign period (29th June - 16th July 2016) from the GEOS-Chem model. Significant emission of isoprene over the forested regions of southern West Africa are evident.

A comparison between the observed isoprene concentration (DLR Falcon and BAS Twin Otter) and that predicted by the GEOS-Chem model are shown in Figure 4. The observations are by their very nature spotty but in general the model shows reasonable agreement with the measurements, giving some faith in the model’s ability to capture the emission of isoprene into the air over southern West Africa. Table 2 provides a statistical analysis of the observed and modelled isoprene mixing ratios. The model does a good job of simulating at least the broad scale of isoprene concentrations observed.

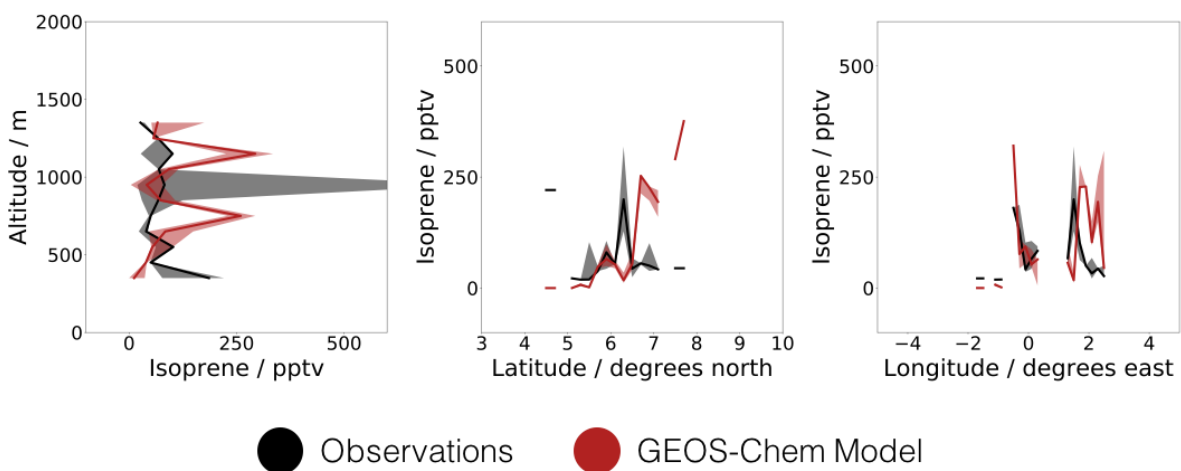


Figure 4. Comparison between modelled and measured isoprene from the Twin Otter and Falcon platform as a function of altitude, latitude and longitude. The solid line represents the median and the shaded regions represent the 25th - 75th percentile range. Simulation performed at a resolution of 0.25° x 0.3125° using the DACCIWA anthropogenic inventory and GFAS biomass burning inventory.

	Observations / pptv	GEOS-Chem Model / pptv
Mean	110.6	101.5
Median	50.4	64.4
Standard Deviation	181.2	98.0
25 th Percentile	35.6	37.5
75 th Percentile	102.6	118.7

Table 2. Observed and modelled isoprene concentrations for the combined DLR Falcon and BAS Twin Otter datasets compared to the GEOS-Chem model.

Within the DACCIWA project *Brosse et al. (2018)* investigated the impact of small scale turbulence on the isoprene concentration over the forests of southern West Africa and concluded that it was a relatively minor source of uncertainty for large scale comparisons.

4.2 Soil NO_x (UPS)

The breakdown of emissions in southern West Africa in the GEOS-Chem model shows that NO released from soils by bacterial activity is thought to be a significant source of NO_x. Observations of soil NO_x fluxes were made at the DACCIWA Savé site and are described in *Pacifico et al. (2018)*. These fluxes were compared to the prediction made by the GEOS-Chem model.

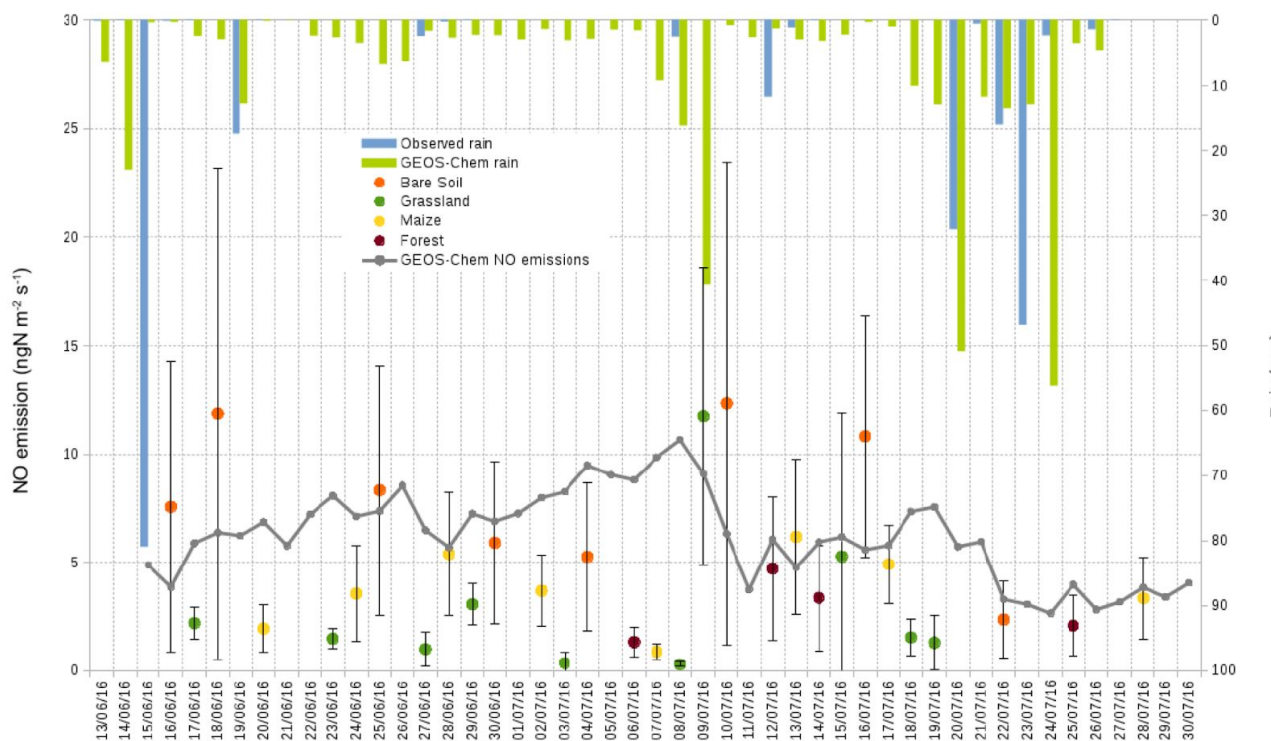


Figure 5. Taken from *Pacifico et al. (2018)*. Emissions of NO from soil as measured from different landscapes (dots) and by the GEOS-Chem model. Rainfall at the sites and from the model is also included. The model emissions are based on the parameterization of *Hudman et al. (2012)*.

The model emissions of NO appear to be relatively consistent with the observations. Over the month of the DACCIWA campaign the model and measurements (scaled up) give relatively similar

results for soil NO_x emissions for Benin with observations suggesting 1.17 ± 0.6 GgN/month and the model giving 1.44 GgN/month.

5 Evaluation of biomass burning emissions

During the summer months in southern West Africa, the monsoonal flow leads to regular rainfall and so local biomass burning is suppressed. However, there is extensive biomass burning in central Africa.

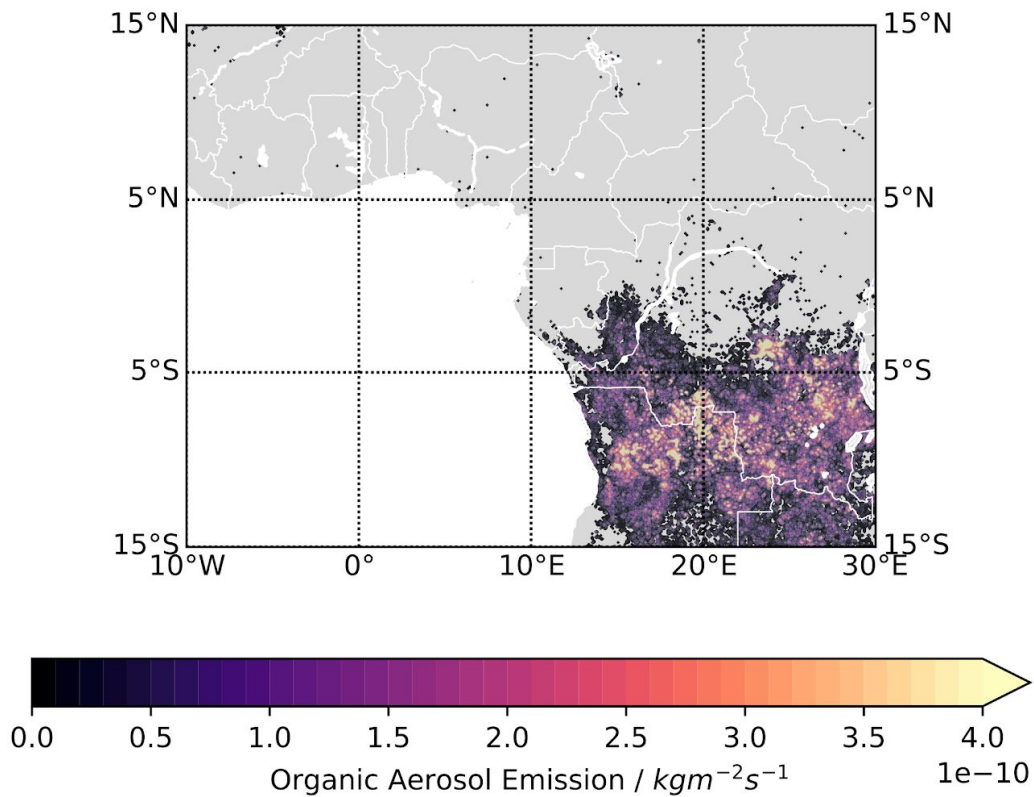


Figure 6. Average GFAS biomass burning emissions of organic aerosol for June-July 2016. There is very little biomass burning over southern West Africa and extensive burning in the Democratic Republic of Congo, Angola and Zambia.

This results in enormous emissions of pollutants into the atmosphere. These emissions are transported in the prevailing easterlies into the Gulf of Guinea where they can go on to impact southern West Africa and then the DACCIWA region.

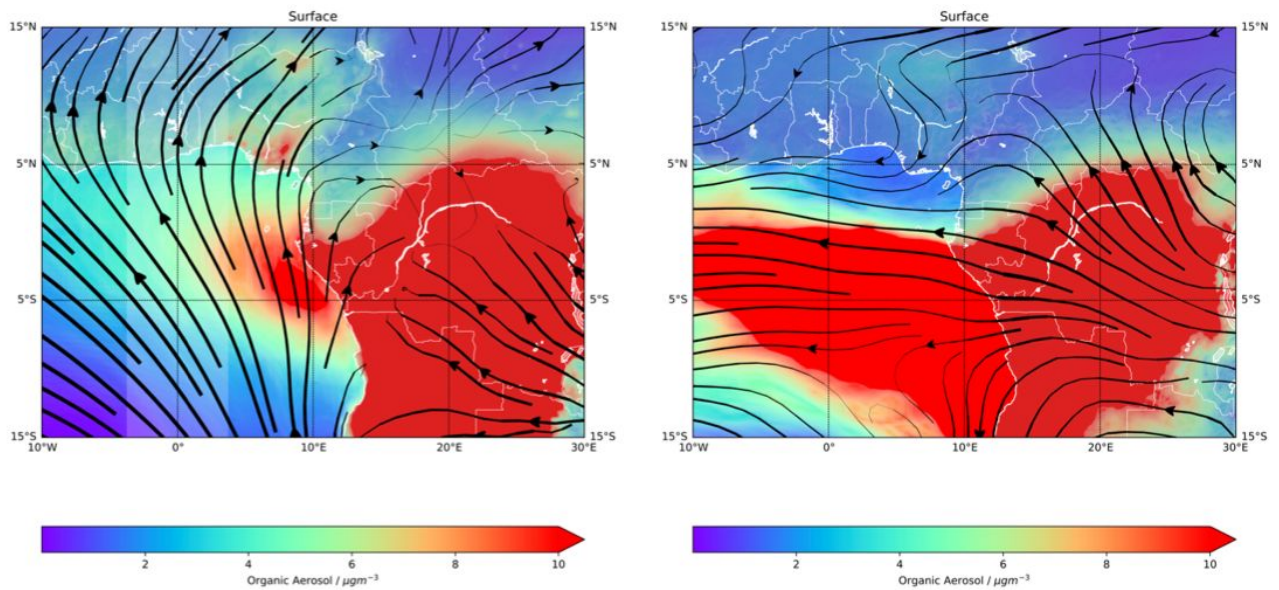


Figure 7. Organic Aerosol mass concentrations (colours) as calculated by the NASA GEOS Nature simulation averaged for 15th June to 15th July at the surface (left) and at 750 hPa (right). Stream lines show the mean horizontal transport in the period, showing rapid east to west transport of organic aerosol at 750 hPa. At the surface, some of this biomass burning aerosol is transported northwards in the monsoonal flow into the DACCIWA domain.

5.1 CHIMERE (UPMC)

The transport pathways for central Africa biomass burning to influence southern West Africa is described extensively in *Menut et al. (2018)*.

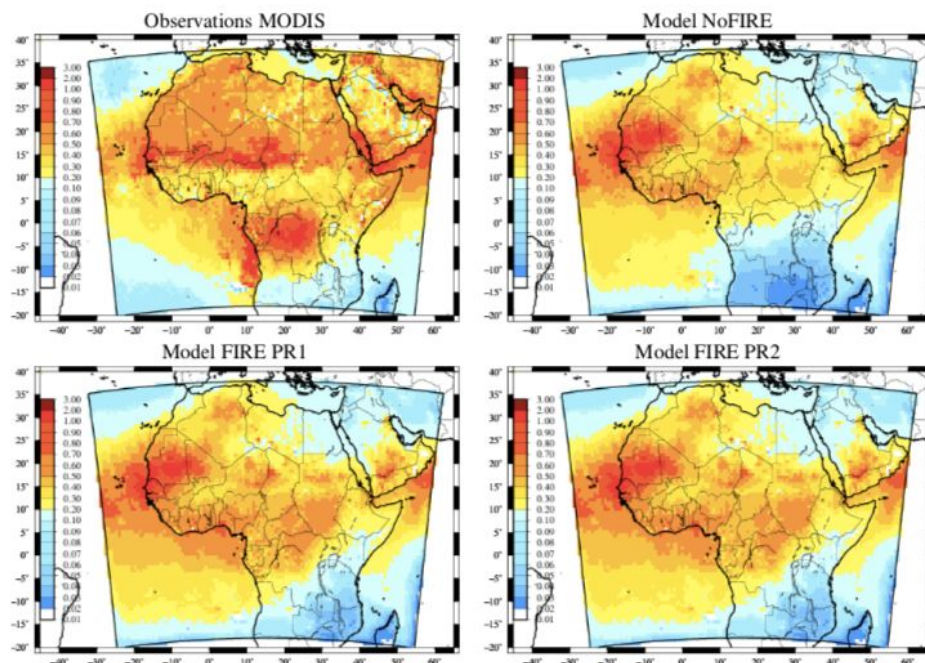


Figure 5. Monthly averaged horizontal distribution of AOD (550 nm) for MODIS and CHIMERE simulations NoFIRE, FIRE PR1, and PR2.

Figure 8. Taken from *Menut et al. (2018)*. This shows the observed aerosol AOD (top left) and a number of model simulations with either no biomass burning (top right) or different assumptions about the biomass burning (bottom panels) for the summer of 2014.

Menut et al. used the APIFLAME biomass burning emissions model (*Turquety et al., 2014*) within the CHIMERE model (see Section 3.2) and concluded that the assumed emissions height of the

biomass burning played a significant role in determining the influence of the central African biomass burning on southern West Africa.

5.2 GEOS-Chem (UoY)

In this study (currently unpublished) the role of biomass burning in controlling the concentration of pollutants in West Africa uses the GFAS emissions from ECMWF within the GEOS-Chem framework. Simulations were run with and without emissions at 2° x 2.5° global horizontal resolution. Figures 9 and 10 show the influence of biomass burning on a number of primary and secondary compounds in the region during the DACCIWA period.

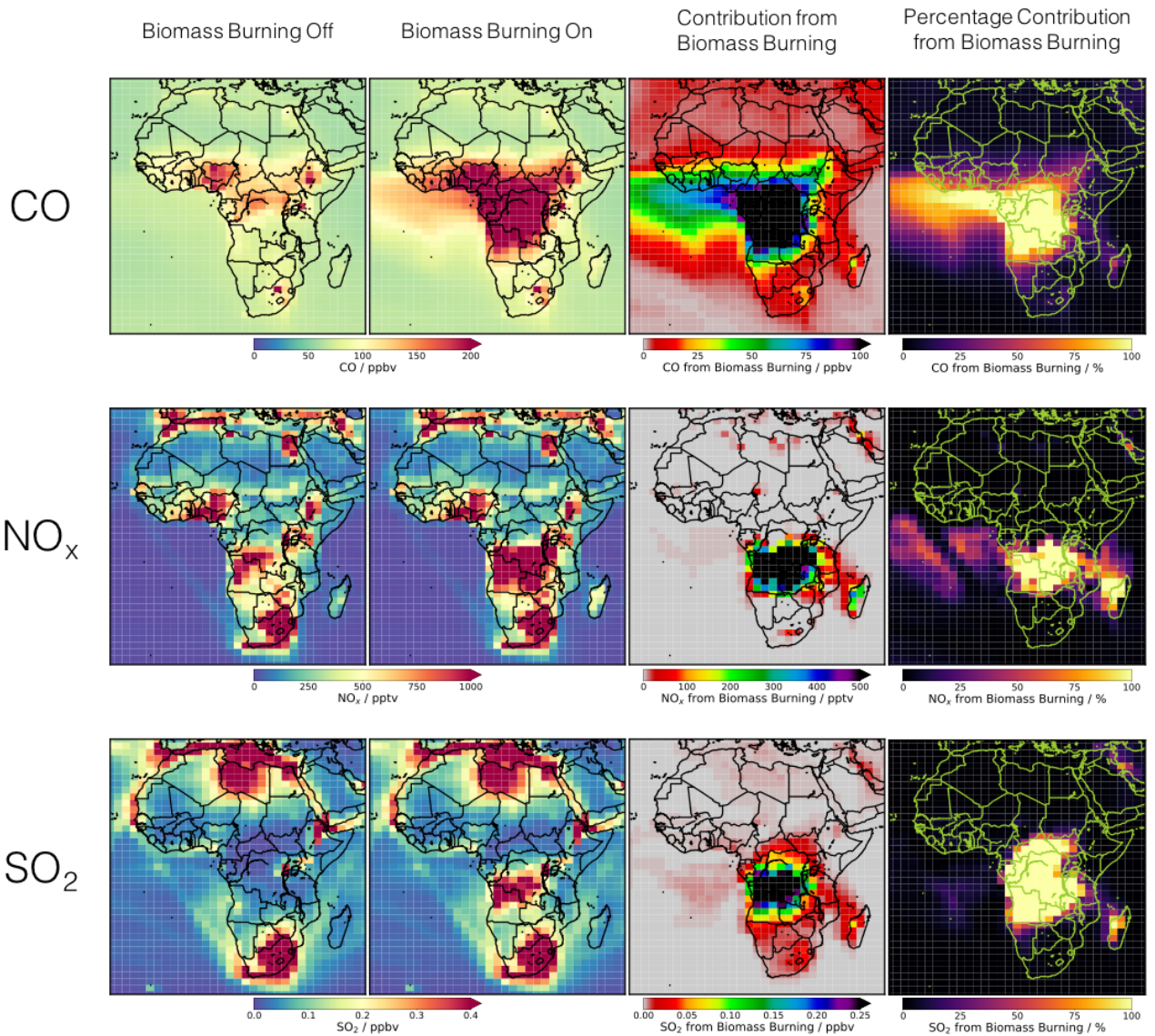


Figure 9. Surface concentration of primary pollutants (CO, NO_x, SO₂ from top to bottom) with biomass burning off, and on, the difference between the two and the ratio within the GEOS-Chem model between the 29th June and the 16th July 2016. The maps are calculated using the 2° x 2.5° global simulation.

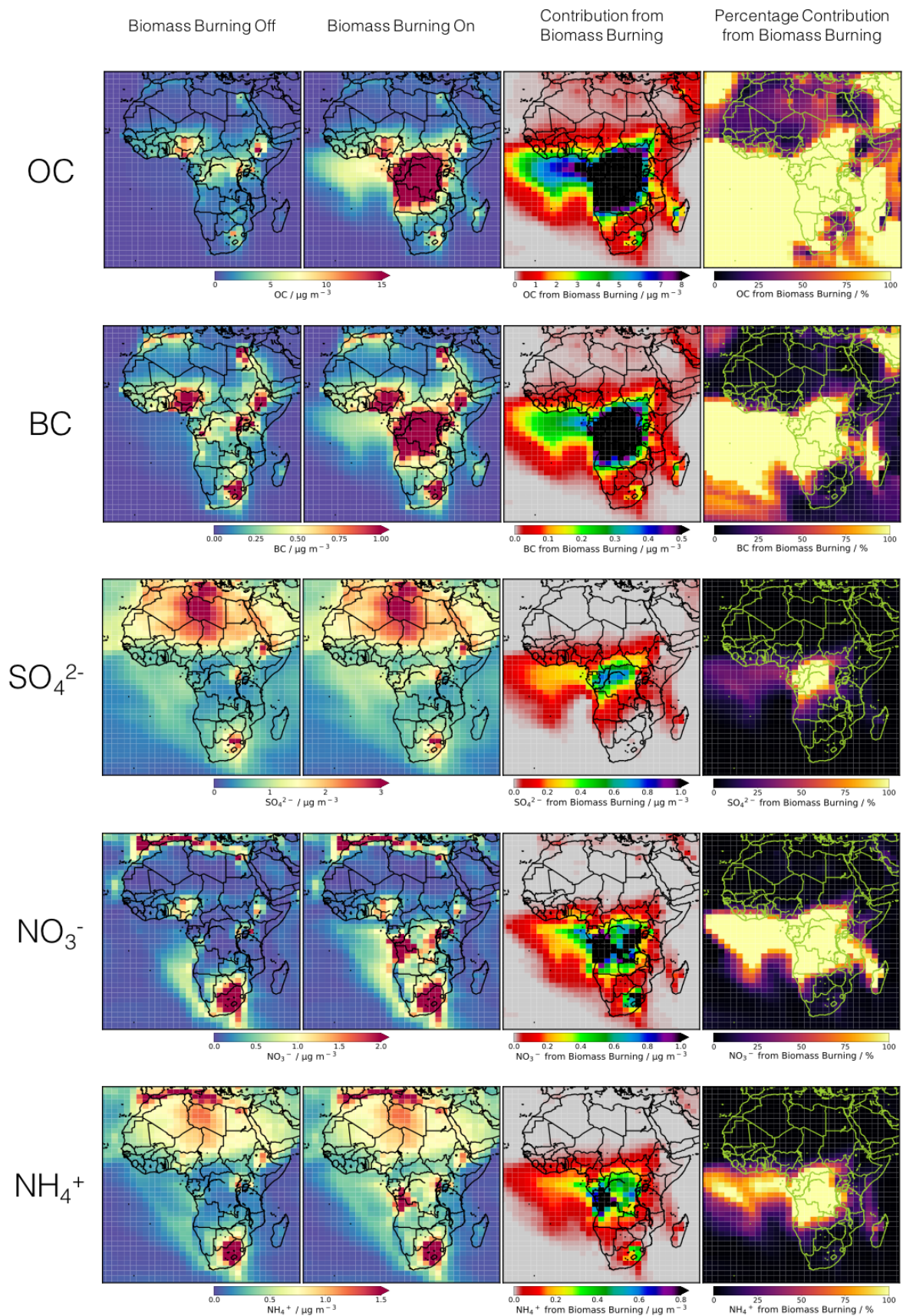


Figure 10. Surface concentration of aerosols (OC, BC, SO_4^{2-} , NO_3^- , NH_4^+ from top to bottom) with biomass burning off, and on, the difference between the two and the ratio within the GEOS-Chem model between the 29th June and the 16th July 2016. The maps are calculated using the $2^\circ \times 2.5^\circ$ global simulation.

The comparison of model predictions with and without biomass burning within the GEOS-Chem model against the DACCIIWA aircraft observations is shown in Figure 11. For some species (OC, BC, CO) biomass burning makes a significant contribution (~50%) to the observed concentration of pollutants. For others it makes little or no contribution (NO_x , SO_2). The impact of biomass burning on critical secondary pollutants (O_3 and $\text{PM}_{2.5}$) is shown in Section 7.1 of this report.

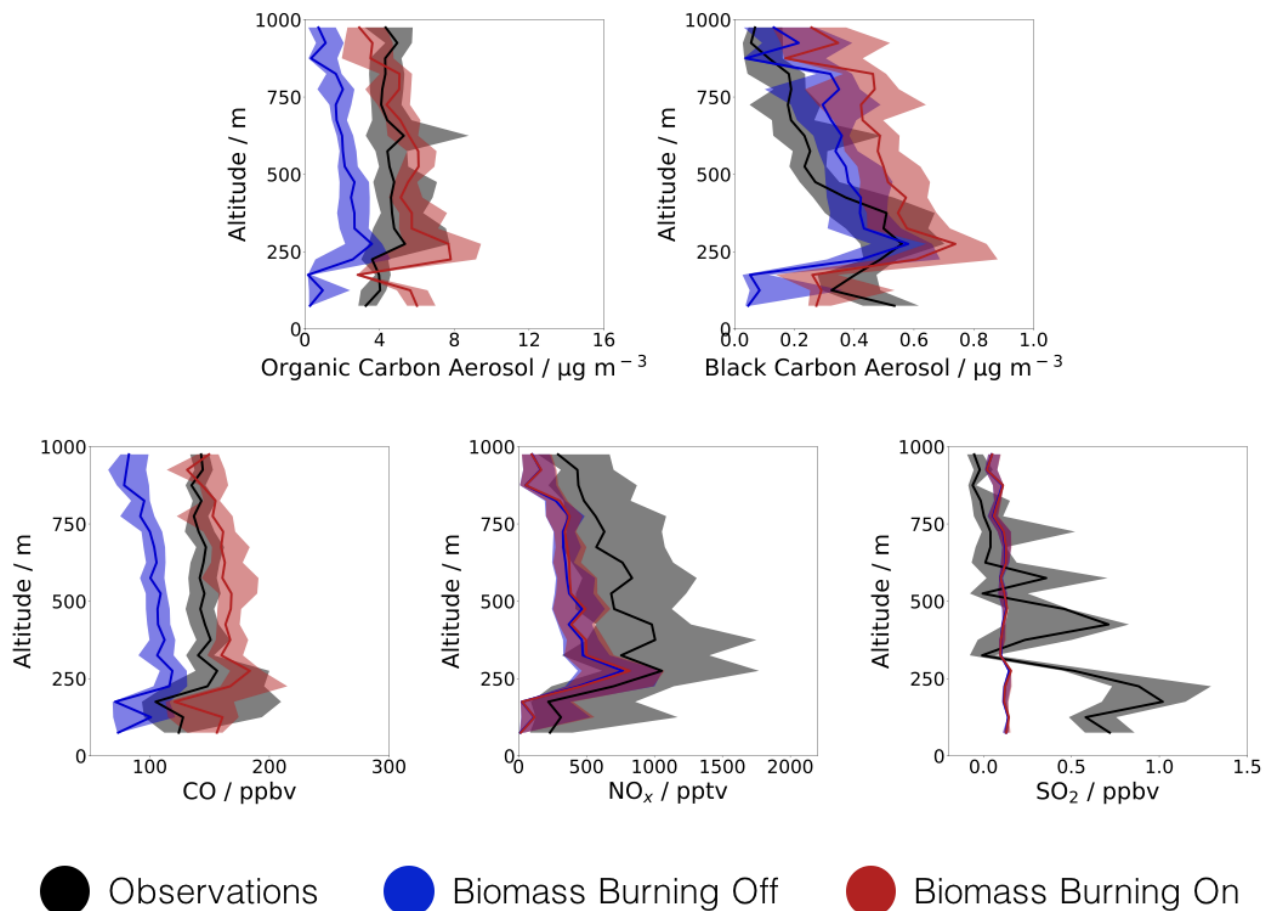


Figure 11. Comparison of mean vertical profiles (0-1000m) from the DACCIIWA aircraft data with the GEOS-Chem model output using the DACCIIWA anthropogenic emissions inventory, with and without the GFAS biomass burning inventory.

6 Evaluation of anthropogenic emissions

There are two studies which have evaluated southern West African anthropogenic emissions by using a chemistry transport model and comparing its results to observations. One using the CHIMERE model (Section 6.1) and one using GEOS-Chem (Section 6.2). Two other studies have investigated this in different ways. The ECHAM6-HAM2 (Section 6.3) model is used to evaluate how different emissions inventories impact the concentrations of $\text{PM}_{2.5}$ over southern West Africa, and one (Section 6.4) which directly evaluated emissions of VOCs in the region.

6.1 CHIMERE (UPMC)

In order to evaluate the HTAP anthropogenic inventory of the EDGAR team (*Janssens-Maenhout et al., 2015*), two anthropogenic emission scenarios were compared against aircraft measurements from the DACCIIWA campaign using the CHIMERE model (*Mailler et al., 2017*). Two ATR flights are examined (3rd July 2016, between 0900 and 1300 UTC and the 5th July 2016, between 0800 and 1000 UTC). The flight path of the aircraft and the NO_2 concentrations observed are shown in

Figure 12. The CHIMERE model is run with both the standard EDGAR emissions and with substantially increased emissions for all anthropogenic species (x10).

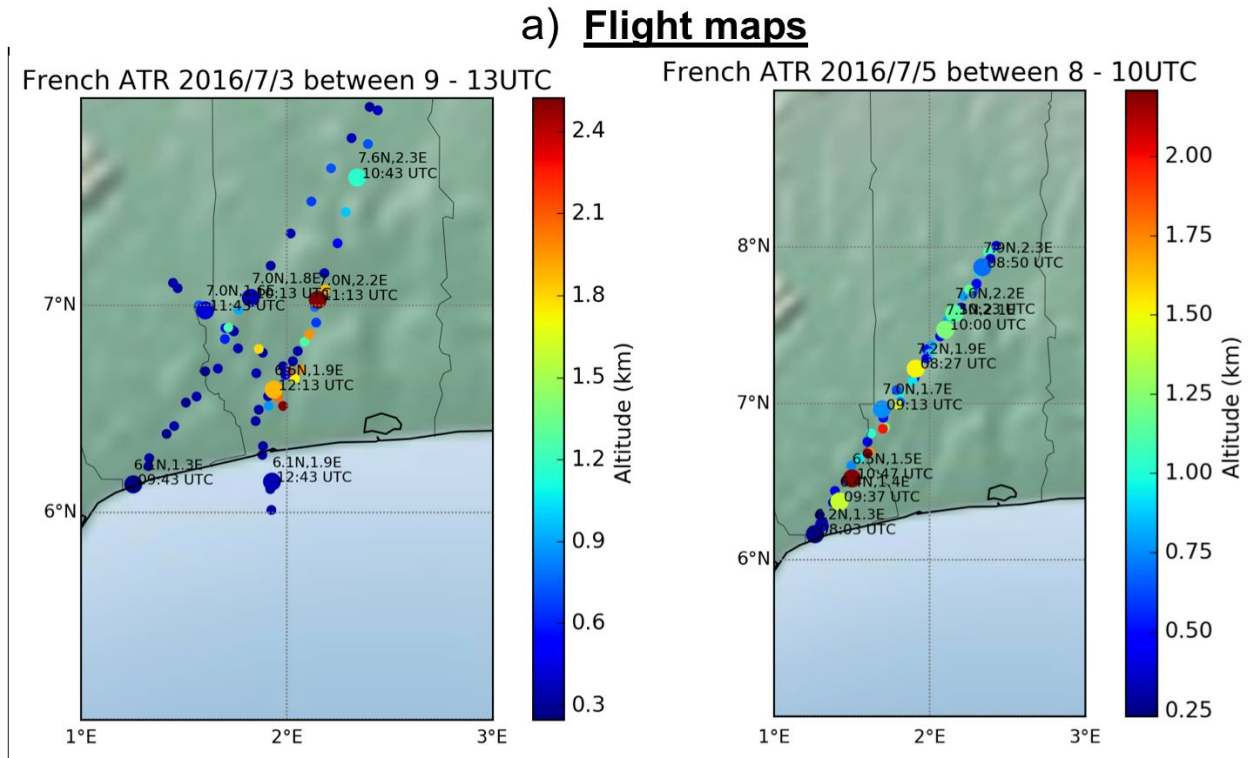
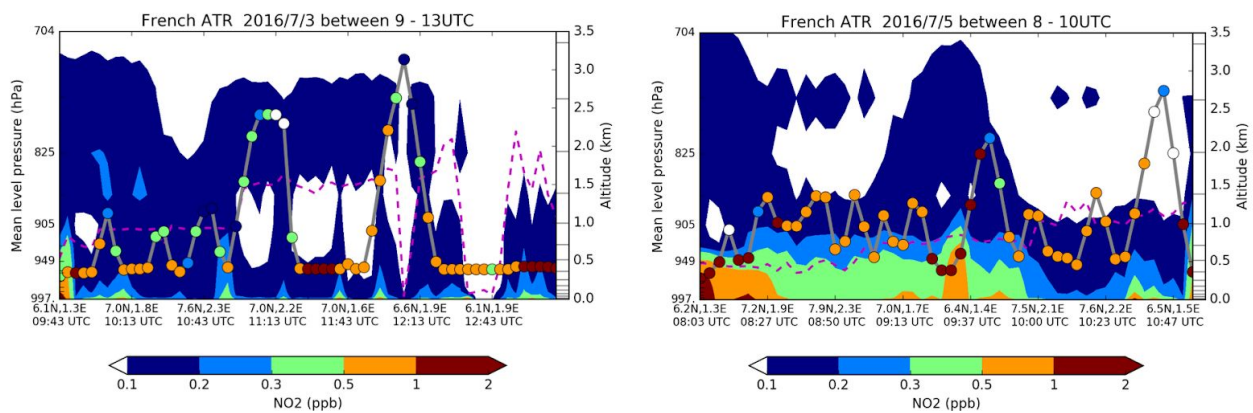


Figure 12. Flight path of the the ATR aircraft on the 3rd July 2016 (left) and 5th July 2016 (right). Coloured dots represent the altitude.

b) NO₂ concentration observed and modeled with HTAP inventory



c) NO₂ concentration observed and modeled with HTAP inventory multiplied by 10

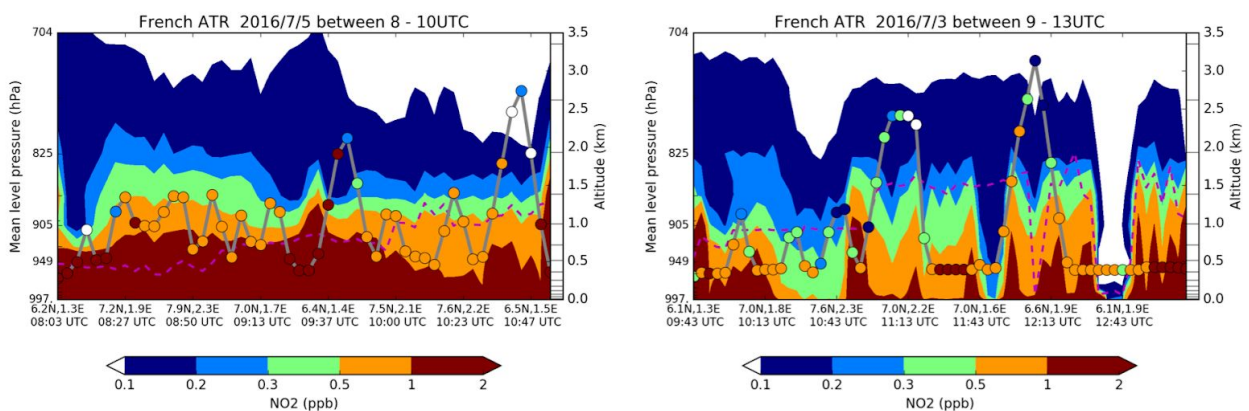


Figure 13. Modelled concentration of NO₂ shown as a function of altitude and time for the two ATR flights on the 3rd July 2016 (left) and 5th July 2016 (right). Contours indicate modelled concentrations, coloured dots indicate the observed NO₂ concentration. Upper plots show the modelled altitude - time distribution using the standard HTAP anthropogenic emissions for the two flights. The lower plots show same but using the standard HTAP anthropogenic emissions multiplied by 10.

Figure 13 shows a comparison between the model and measured NO₂ concentration along the flight track for both emissions scenarios. This shows that the model's fidelity is much improved by the substantial increase in the anthropogenic emissions.

Further details can be seen in Figure 14. This again shows direct comparison between the measured and modelled CO, NO₂ and O₃ for the flight on the 5th July 2016 for the simulation with the standard EDGAR emissions and with emissions increased by a factor of 10. For the NO₂ the comparison with the observations is improved substantially with the increase by a factor of 10. However increasing the CO emissions by this factor makes the model substantially overestimate CO concentrations. This also has the tendency to overestimate O₃ concentrations along the flight.

French ATR 2016/7/5 between 8 - 10UTC

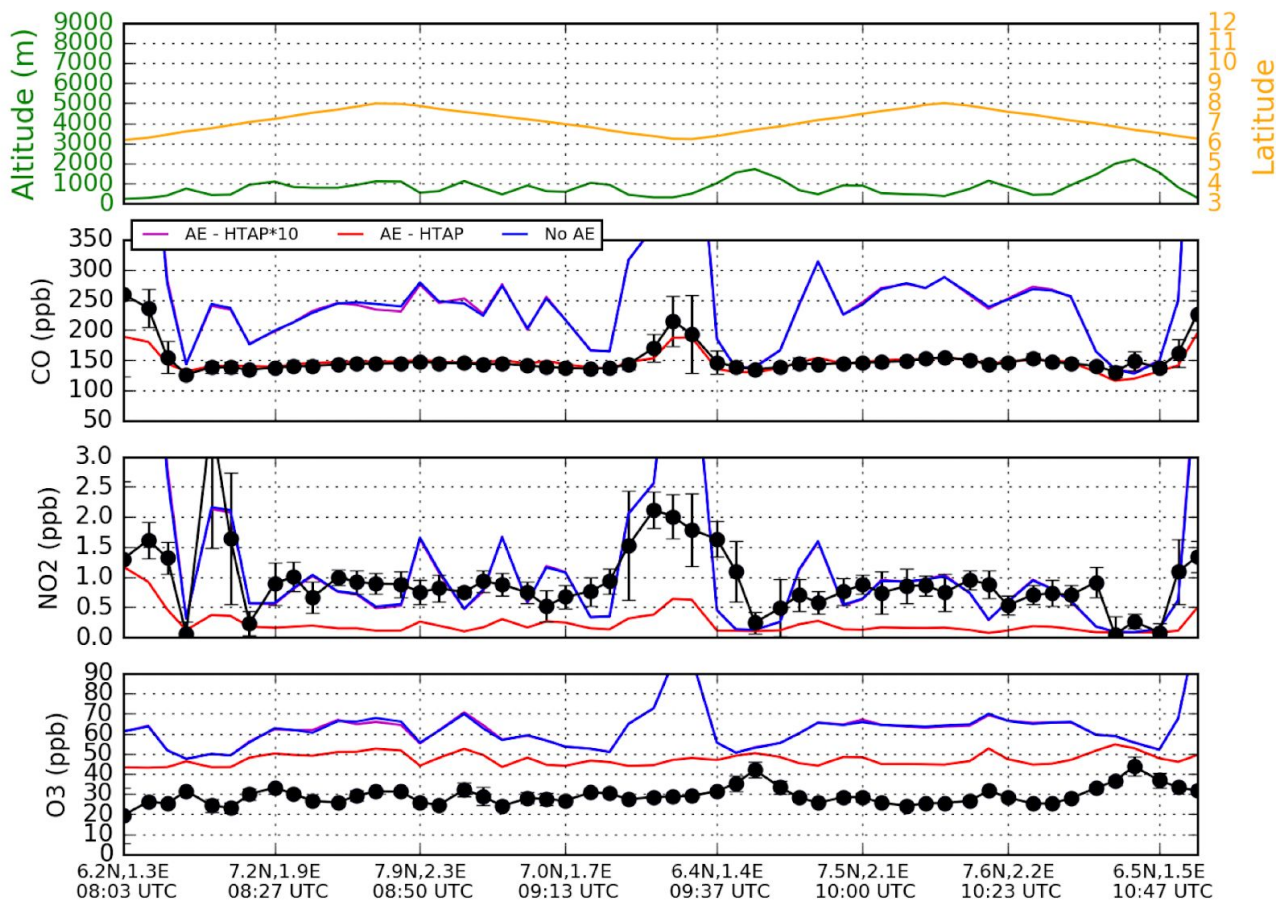


Figure 14. Time series of latitude and altitude, and CO, NO₂ and O₃ mixing ratio made from the ATR aircraft on the 5th July 2016 together with the two simulation results of the CHIMERE model. Standard emissions in blue and x10 anthropogenic emissions in red.

This would suggest that the quality of the EDGAR emissions within the DACCIWA period is not just one of overall underestimated activity but also in the emissions ratio. From this study it would appear that the emissions ratio between NO_x and CO would need to be changed within the model to get agreement. Dynamical explanations may explain some of the differences between the model and the measurements. The concentrations calculated are sensitive to the boundary layer mixing / vertical mixing within these morning periods, when the boundary layer is stable and low. But even if the mixing is badly constrained, it seems unlikely that a dynamical effect alone can explain the systematic underestimation and the low modeled values, including near the surface.

6.2 GEOS-Chem (UoY)

The GEOS-Chem model has been run along all of the flights made by all of the aircraft to compare with observations. In order to emphasise the anthropogenic component of the emissions, comparisons have only been made with those data over the lowest most 1000 m over the major cities (shown in Figure 15).

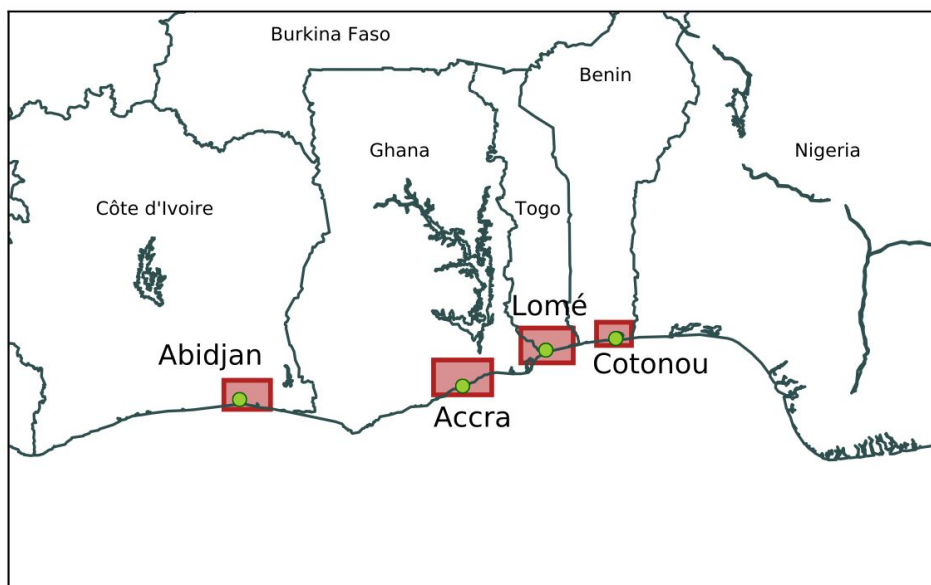


Figure 15. Locations around the four major cities surveyed during the aircraft campaign for which data has been used to generate the model-observation comparisons shown in Figures 16, 17 and 18.

We compare the mean profile (0-1000 m) observed by all aircraft over the major cities in the region (Abidjan, Accra, Lomé and Cotonou) with the equivalent profiles calculated by the model running 3 different emissions scenarios: EDGAR emissions, DACCIWA emissions and the DACCIWA emissions scaled to get better agreement with the observations. The magnitude of the scalings for each subject is shown in Table 3 along with scaling used.

The model run with the DACCIWA emissions show a significantly better comparison with observations. NO_x, black carbon and organic aerosol all increase significantly and become much closer to the observed concentrations. SO₂ concentrations however, drop and so are significantly lower than those observed. Simulated concentrations of sulfate and ammonium aerosol remain at half those observed.

We scale the DACCIWA emissions to get better agreement between modelled and observed primary species (CO, BC, OC, NO_x, SO₂). The scalings applied are given in Table 3. This is a simple scaling of the emissions in the whole of the domain. A significant scaling (x10) of the SO₂ is necessary to get agreement, but better agreement is possible. However, even with this increase in SO₂ emissions, sulfate concentrations are still underestimated as are ammonia emissions. Nitrate is now significantly overestimated. This suggests that even Africa specific emission inventories may underestimate the current emissions inventories for the region, and for some species significantly.

	Observations	Model / Observation Ratio			Scale Factors used for DACCIWA "Improved"
		EDGAR	DACCIWA	DACCIWA "Improved"	
CO	149 ppbv	0.94	1.14	1.16	-
NO _x	827 pptv	0.40	0.73	1.04	1.4 (Anthropogenic)
SO ₂	0.52 ppbv	0.51	0.28	1.18	10 (Anthropogenic)
Organic Carbon Aerosol	4.59 µg m ⁻³	0.29	0.80	1.32	-
Black Carbon Aerosol	0.49 µg m ⁻³	0.49	1.24	1.24	-
Sulfate Aerosol	2.19 µg m ⁻³	0.51	0.42	0.57	-
Nitrate Aerosol	0.29 µg m ⁻³	0.72	1.27	1.97	-
Ammonium Aerosol	0.82 µg m ⁻³	0.48	0.46	0.67	-

Table 3. Measured median concentrations of pollutants in lowest most 500 m over the DACCIWA cities. Ratios between model and measured median concentrations for a number of emissions scenarios.

The sulfate-ammonia-nitrate system has a complex response. Despite both the sulfur and nitrate precursors (SO₂, NO_x) showing relatively good agreement after scaling the sulfate is underestimated and the nitrate over estimated. There is no simple answer to this. An increase in the rate of SO₂ to sulfate conversion coupled to an increase in the SO₂ emissions would maintain the same SO₂ concentration but also lead to enhanced sulfate concentrations. There is currently much debate about mechanisms that can achieve this (see for example *He et al., 2015*) with both mineral dust and NO₂ candidates for accelerating this conversion.

Secondary pollutants such as ozone, also change in response to these changes in the primary emissions. Figure 17 shows the vertical profile of O₃ calculated over the coastal cities. Going from the EDGAR emissions to the 'improved' DACCIWA emissions leads to an increase in ozone of around 5 ppbv, or around 20%. The model overestimates the ozone at the surface. This may reflect an overestimate in the surface ozone concentrations over the ocean. We note that *Sherwen et al. (2017)* found ~8 ppbv difference in the surface ozone concentrations in this region with and without halogen chemistry. The current model only includes the chemistry of bromine and so this overestimate in the surface concentrations may reflect this missing halogen chemistry in this model

simulation. The impact of the different emissions inventories on the ozone over the cities is rather minor.

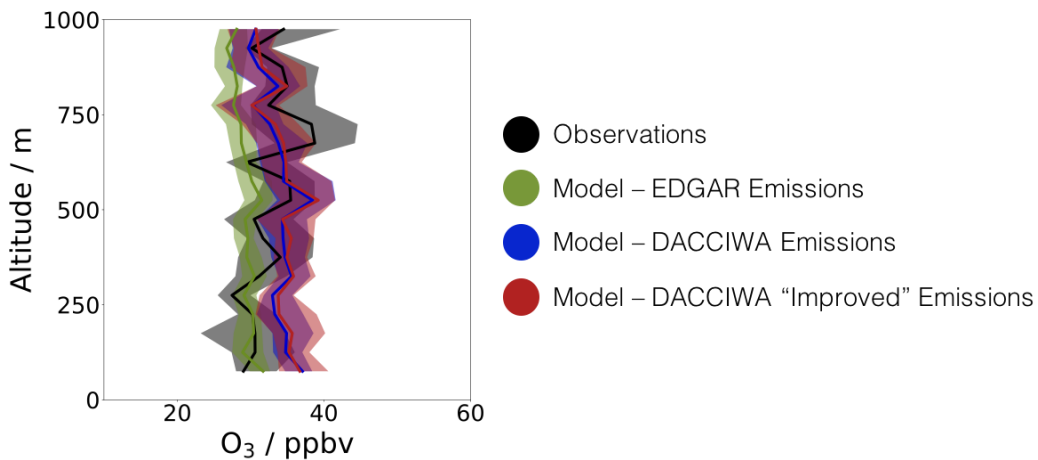


Figure 17. Measured and modelled O_3 concentrations over the DACCIWA cities with the EDGAR, DACCIWA and the DACCIWA 'Improved' emissions.

Figure 18 shows the vertical profile of $PM_{2.5}$ calculated from the GEOS-Chem model. This takes into account the mass of all of the aerosol tracers (sulfate, nitrate, ammonium, black carbon, organic carbon, dust, sea salt) and include additional mass due to the uptake of water to those aerosols (http://wiki.seas.harvard.edu/geos-chem/index.php/Particulate_matter_in_GEOS-Chem). The aircraft did not carry an instrument to measure $PM_{2.5}$ in isolation so we do not compare to observations. However we note that the $PM_{2.5}$ mass is consistent with on ground based observations of $20-30 \mu g m^{-3}$ (see for example *Djossou et al., 2018*) only when the Improved DACCIWA emissions are used. Use of the EDGAR emissions likely underestimates the $PM_{2.5}$ over the coastal DACCIWA cities by an order of 4.

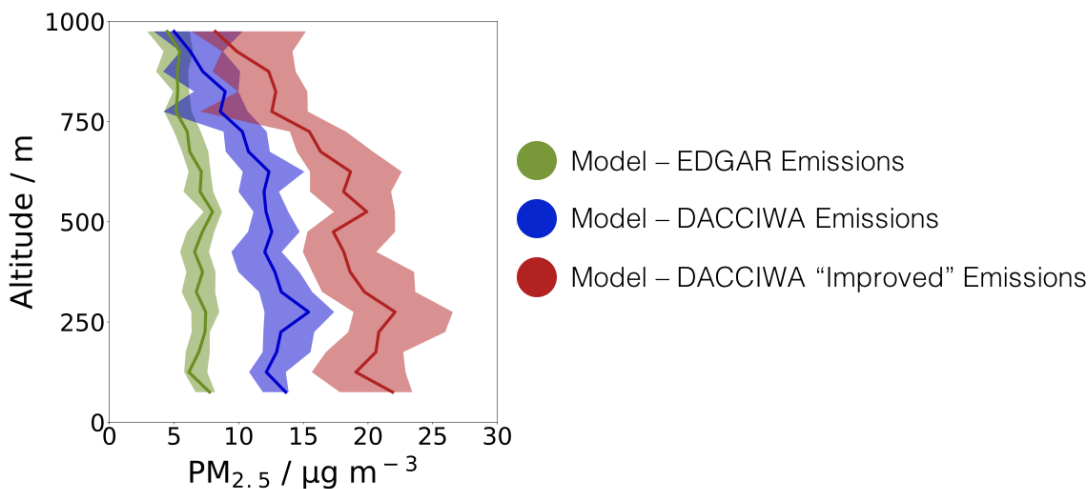


Figure 18. Modelled $PM_{2.5}$ concentrations over the DACCIWA cities with the EDGAR, DACCIWA and the DACCIWA 'Improved' emissions. No direct measurement of $PM_{2.5}$ was made from the aircraft.

6.3 ECHAM6-HAM2 (ETHZ)

Comparison between a climate model such as ECHAM-HAM2 and the DACCIWA observations is difficult due to the meteorology in the model not directly aligning with the actual meteorology. Instead the impact of different emissions estimates within the literature are compared. Table 4 shows the emissions used in these simulations.

Simulation name	Anthropogenic emissions	Biomass burning emissions
accmip	ACCMIP (Lamarque et al., 2010)	ACCMIP (Lamarque et al., 2010)
accmip_gfas	ACCMIP (Lamarque et al., 2010)	GFAS (Heil et al., 2010)
htap	HTAP (http://edgar.jrc.ec.europa.eu/htap_v2/)	GFAS (Heil et al., 2010)
ceds	CEDS (http://www.globalchange.umd.edu/ceds/)	GFAS (Heil et al., 2010)
dacsiwa	DACCIWA (WP2, deliverable 2.1)	GFAS (Heil et al., 2010)
0.25dom	HTAP (http://edgar.jrc.ec.europa.eu/htap_v2/) Emissions from domestic sector are multiplied by 0.25	GFAS (Heil et al., 2010)

Table 4. Emissions used in the simulations. GFAS biomass burning emission fluxes are multiplied by a factor of 3.4 as recommended by Kaiser et al. (2012).

The most important sector for aerosol emission in southern West Africa is the domestic sector (Figures 19 – 21). To explore the model sensitivity to this sector, a sensitivity experiment is performed which reduces the emissions from the domestic sector to a quarter of the htap2.0 prescribed emission flux. This explores whether a drastic reduction of emissions from the domestic sector will improve the air quality in south West Africa.

Figure 19 shows the differing emissions of SO₂ from the different emissions datasets for the DACCIWA region of West Africa.

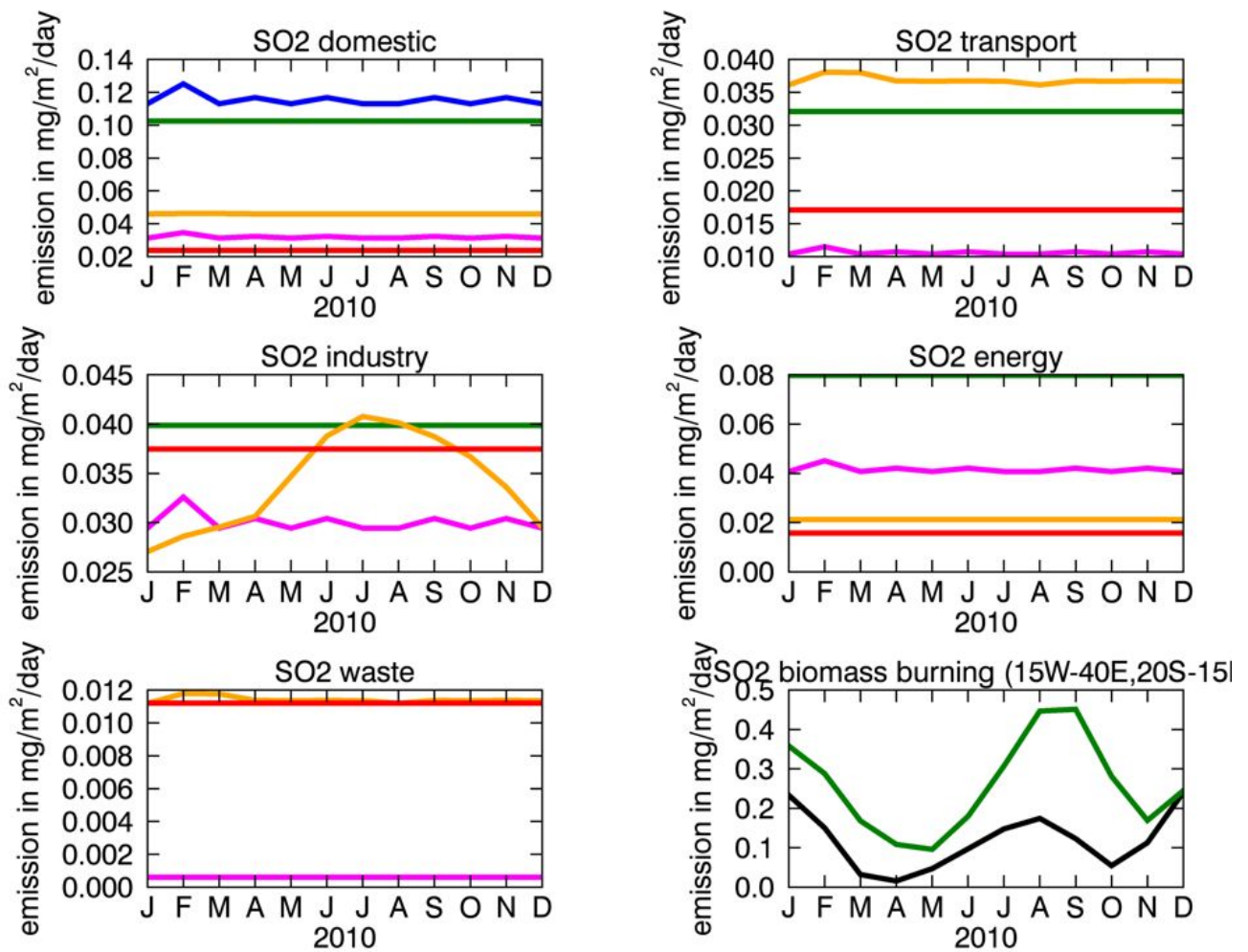


Figure 19. Regional averaged (anthropogenic: 15° W – 15° E, 5° N – 15° N, biomass burning: 15° W – 40° E, 20° S – 15° N) SO₂ emission flux split into different sectors for 2010 (black – accmip, green – accmip_gfas, orange – ceds, red – dacciwa, blue – htap2.0, magenta – 0.25dom).

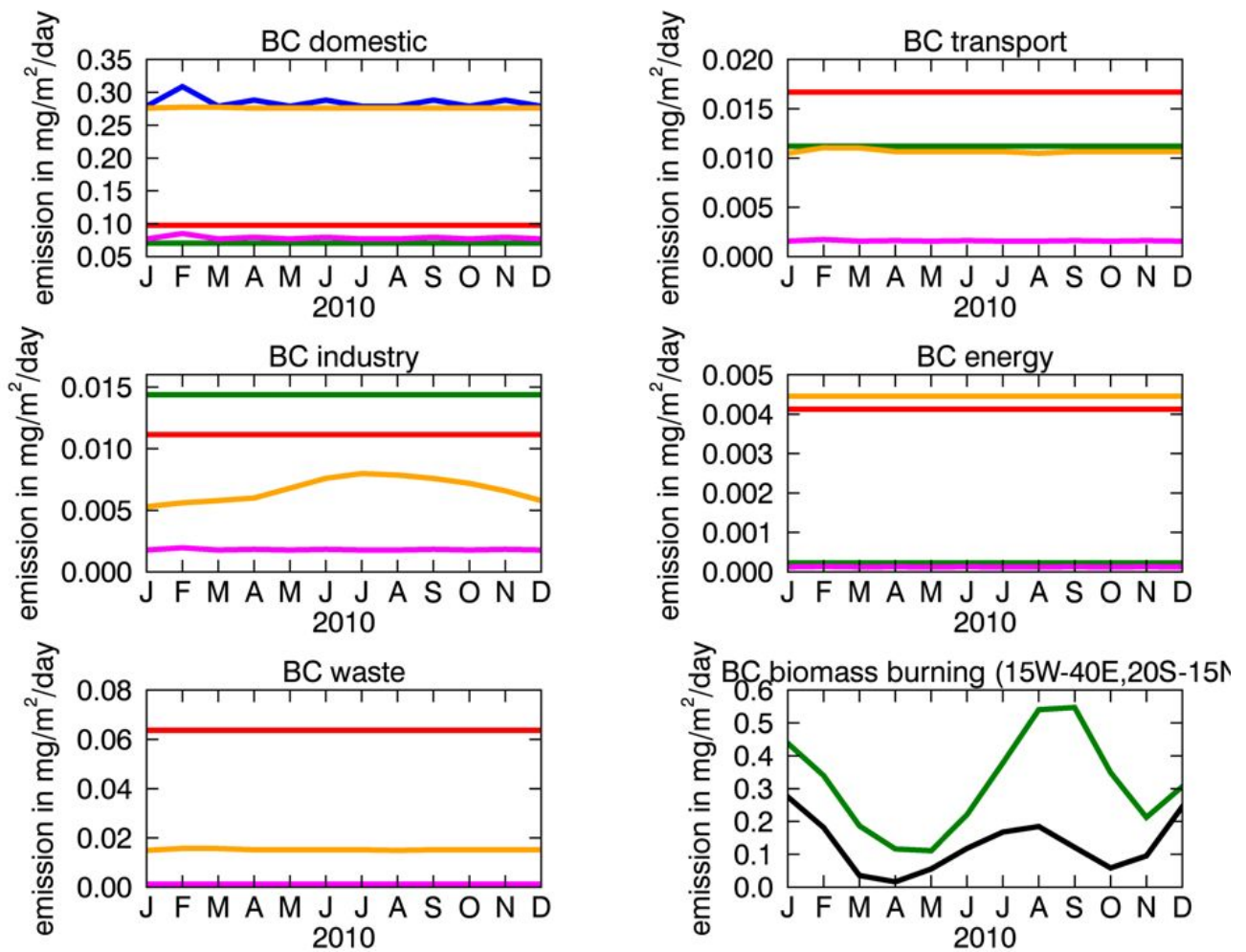


Figure 20. Regional averaged (anthropogenic: 15° W – 15° E, 5° N – 15° N, biomass burning: 15° W – 40° E, 20° S – 15° N) black carbon emission flux split into different sectors for 2010 (black – accmip, green – accmip_gfas, orange – ceds, red – dacciwa, blue – htap2.0, magenta – 0.25dom).

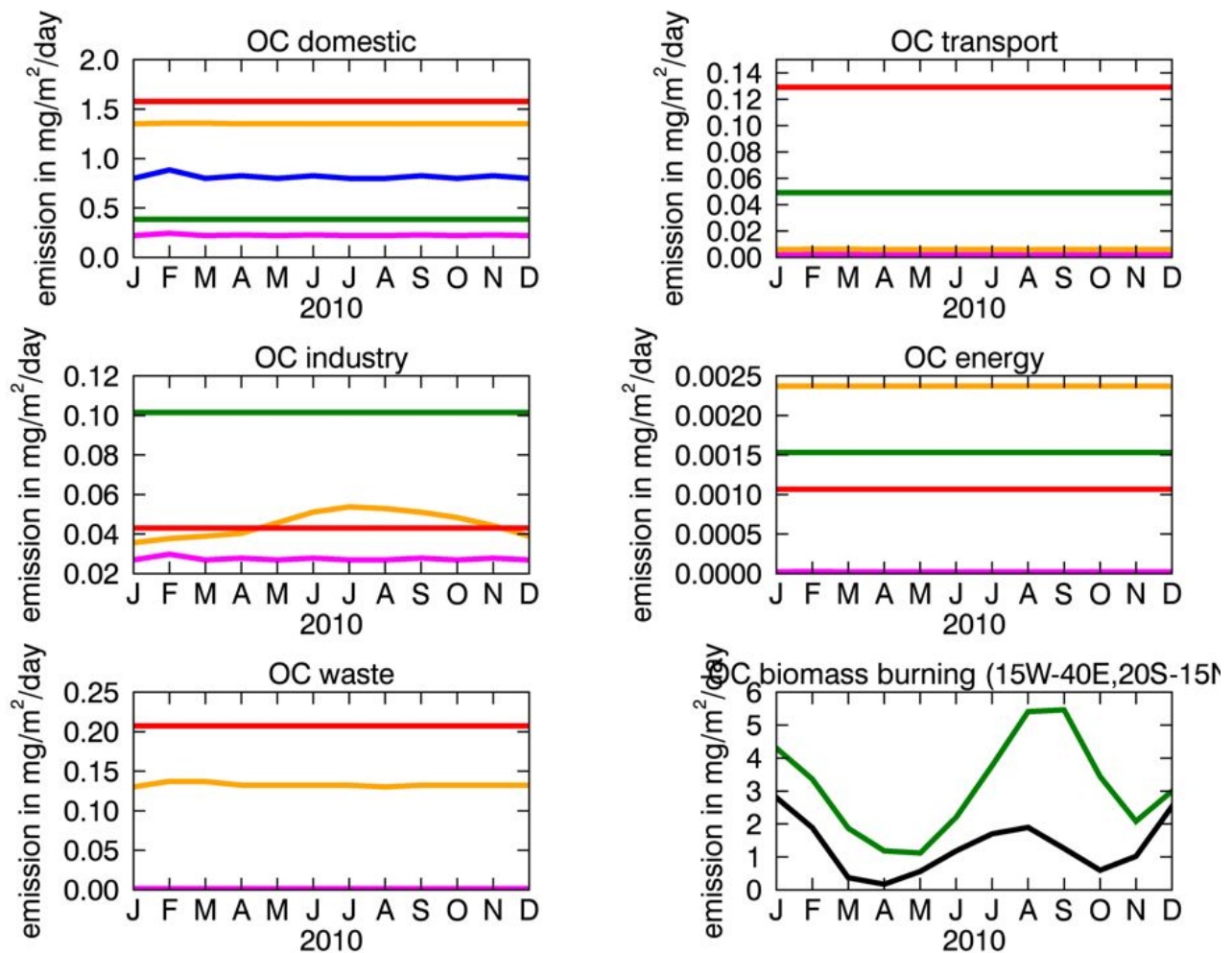


Figure 21. Regional averaged (anthropogenic: $15^\circ \text{W} - 15^\circ \text{E}$, $5^\circ \text{N} - 15^\circ \text{N}$, biomass burning: $15^\circ \text{W} - 40^\circ \text{E}$, $20^\circ \text{S} - 15^\circ \text{N}$) organic carbon emission flux split into different sectors for 2010 (black – accmip, green – accmip_gfas, orange – orange-ceds, red – dacciwa, blue – htap2.0, magenta – 0.25dom).

6.3.2 Impact on air quality

Particles with diameter less than $2.5 \mu\text{m}$ (denoted $\text{PM}_{2.5}$ in the following) can penetrate deeply into the lung, where they impair the lung function. In terms of air quality, $\text{PM}_{2.5}$ is therefore an important measure. The $\text{PM}_{2.5}$ concentration is very high in southern West Africa (Figures 22 and 23). Depending on the applied emission inventory the $\text{PM}_{2.5}$ concentration varies between $120 \mu\text{g}/\text{m}^3$ and $210 \mu\text{g}/\text{m}^3$ in winter. During summer, the $\text{PM}_{2.5}$ concentration is lower, between $7 \mu\text{g}/\text{m}^3$ and $18 \mu\text{g}/\text{m}^3$. The simulated annual mean $\text{PM}_{2.5}$ concentration is $50\text{--}70 \mu\text{g}/\text{m}^3$. These values are very much above the recommendation of $10 \mu\text{g}/\text{m}^3$, which is given by the World Health Organization. This is especially alarming since the model results represent regional averages. City plumes are not resolved in the coarse resolution of $200 \times 200 \text{ km}$ of our model simulations. Therefore, the concentration in the cities could be even higher.

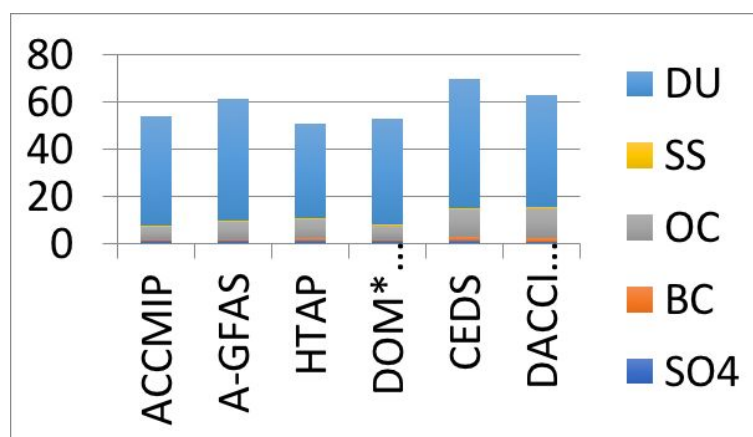


Figure 22. Multi-annual mean $PM_{2.5}$ surface concentrations in $\mu g m^{-3}$, averaged over the DACCIWA domain ($8^{\circ} W - 8^{\circ} E$, $5^{\circ} N - 10^{\circ} N$) with the differing emissions datasets. DU: dust, SS: Sea Salt, OC: Organic Carbon, BC: Sulfate.

Dust particles represent a large portion of the high aerosol load. They are emitted in the Sahara and then transported by the north-easterly Harmattan wind to the coast. The wind mainly occurs between the end of November and the middle of March. This is the time when the coast is affected most by the high dust load (Figure 22). During this time of the year the anthropogenic contribution to the total dust load is small. The differences in the $PM_{2.5}$ concentrations between the performed simulations is caused by changes in dust concentrations. Dust emissions are calculated in dependency of the vegetation cover, wind speed, and soil properties in ECHAM6-HAM2. The changes in the emission fluxes are caused by induced changes in wind speed due to feedbacks between aerosols, radiation and clouds. The wind speed plays a key role in calculating dust emissions. First, a specific (dependent on soil properties) threshold of the friction velocity has to be reached so that dust can be emitted. Second, the dust emission flux is proportional to the cubic of the wind speed. Therefore, small changes in wind speed can have large effects on the simulated dust emission flux. In addition, changes in the circulation affect the transport and deposition of dust particles, which can also result in different amounts of dust at the Guinea Coast. So far, we were not able to identify a consistent pattern in the change of dust concentrations between the simulations. This will be the scope of an upcoming study. But our findings point out the need to understand the dust emission – transport – deposition processes to simulate the aerosol distribution in south West Africa correctly.

During summer (May – October) the contribution of biomass burning and anthropogenic aerosols to the total $PM_{2.5}$ surface concentration is larger. In general, the $PM_{2.5}$ concentration is much lower during summer than during winter because less dust particles are transported to the Guinea Coast. The $PM_{2.5}$ concentration fulfil with approximately $10 \mu g/m^3$ the WHO recommendation in some of the performed simulations. But applying the daccwiwa or ceds emission inventory the recommended value is overshoot also during summertime. The uncertainty induced by the choice of an emission inventory is large during summertime. The difference of calculated $PM_{2.5}$ surface concentrations can vary up to a factor of 2 (September: difference between accmip and daccwiwa, Figure 23).

To answer the question if a decrease in emissions from the domestic sector could result in a significant improvement of the air quality in southern West Africa, we have to focus on simulations “htap” and “0.25dom”. Since during wintertime the dust particles dominate the $PM_{2.5}$ concentrations, there is no improvement in air quality detectable when decreasing emissions from the domestic sector. However, the decrease could even result in a decrease in air quality due to an increase in dust load caused by feedback mechanisms in our model. But since this is only the

result of one model, this finding is not assured and has to be taken with caution! During summertime the decrease in domestic emissions improves the air quality. Since our model runs have a rather coarse simulation it is likely that the improvement in the cities themselves would be much higher than our simulations indicate.

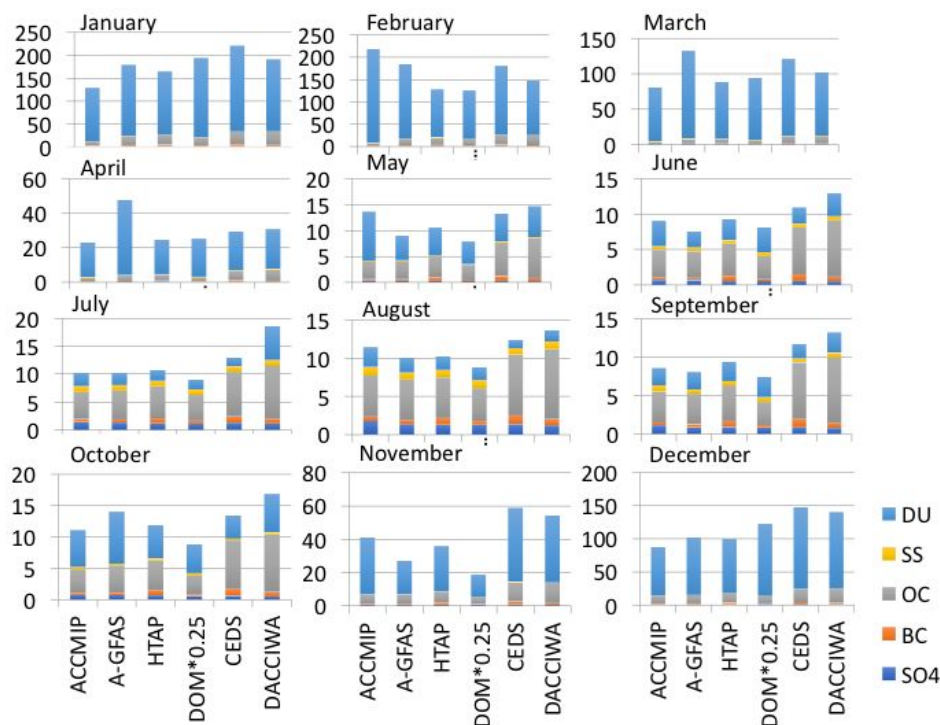


Figure 23. Multi-monthly mean $PM_{2.5}$ concentrations and speciation, averaged over “dacciwa” domain ($8^{\circ} W - 8^{\circ} E, 5^{\circ} N - 10^{\circ} N$) for the different emissions scenarios.

6.4. VOC emissions from cities (UBP)

Assessing VOC emissions and VOC source profiles with emission inventory in Abidjan, West Africa (analysis included in the paper of Keita *et al.*, 2018, accepted in ACP)

Several ground-based field campaigns have been carried out to establish the emission factors of gaseous and particulate pollutants from various representative sources in West Africa, as part of work package 2 (‘Air Pollution and Health’) of the DACCIWA program. Emission sources considered in this study include wood and charcoal burning, charcoal making, open waste burning, and vehicles including trucks, cars, buses and two-wheeled vehicles. Emission factors of total particulate matter, black carbon, primary organic carbon and volatile organic compounds (VOC) have been established. VOCs were actively measured by using sorbent tubes (Tenax and Carbopack). Their analysis was followed by thermal desorption (TD) coupled with a gas chromatograph combined to flame ionization or mass spectrometric detectors. Thus, fifteen VOC species (C5 to C10) were identified and quantified and emission factors estimated for the first time in West Africa. As a whole, the dominant VOC species emitted during EF measurements include toluene, m+p-xylene, 1,2,4-trimethylbenzene (124-TMB), ethylbenzene, o-xylene, 1,3,5-trimethylbenzene (135-TMB) and heptane. These new data have been used to evaluate the emission inventories with Ivory Coast as a first case study. VOC emissions were calculated by combining the new EF and statistical data on activity levels provided by IEA and then compared with those provided by the EDGAR inventory (EDGAR v4.3.2) for the road transport sector. For that purpose, the fifteen VOCs were aggregated according to GEIA VOCs groups (Huang *et al.*,

2017). In Figure 24 the road transport emissions for the year 2012 in Ivory Coast are compared. Notwithstanding the selected number of VOC species, a large discrepancy can be noted between both inventories (Figure 24a): the EDGAR inventory underestimates VOC emissions by a factor of 50. In terms of composition, the main differences are observed for VOC6 group (>C6 alkanes), which presents a greater contribution in the EDGAR inventory. This disparity could also be related to the few VOC species that were analysed for VOC6 group in our study. In contrast, aromatics compounds dominate the updated emission inventory, especially for C8 and C9 compounds (40% and 25%, respectively, Figure 24b). Since the reactivity is different for each species, the inaccuracies in the VOC speciation have also consequences in the estimation of their impacts: the total reactivity is underestimated by a factor of 2 by EDGAR compared with the new emission inventory (Figure 24c).

The scarcity of measurements and sources profile data in Africa were previously pointed out in the development of EDGAR inventory, which leads to consider the priority of this region for future inventory improvements (Huang *et al.*, 2017). Our results show that emissions of anthropogenic VOCs by actual emission inventory are largely underestimated and show the usefulness of in-situ measurements in real conditions to derive realistic emission factors and subsequent emissions of better quality.

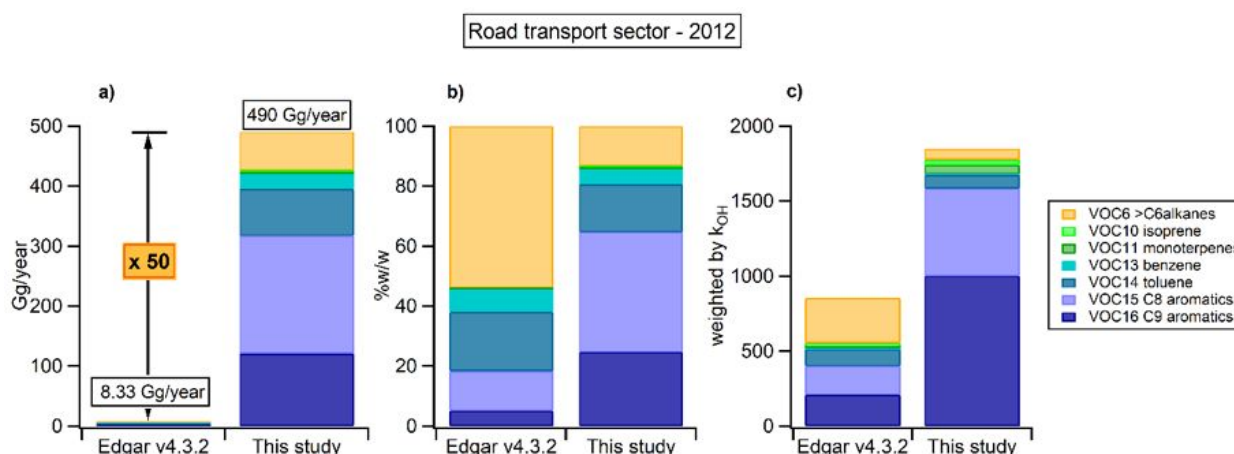


Figure 24. Comparison of VOCs emissions between the new emission inventory (this study) and EDGAR v4.3.2 inventory (Huang *et al.*, 2017) for road transport sector in 2012 in Ivory Coast: (a) absolute emissions in Gg/year, (b) relative mass emissions for selected VOC groups and (c) emission weighted by VOC reactivity for a 100 Gg of VOCs emissions (weighted by k_{OH} mean rate constants)

7 Impacts of emissions on policy relevant species during the DACCIWA campaign period

7.1 Impact of biomass burning (UoY)

In this section we use the GEOS-Chem model to evaluate the impact of the biomass emissions on policy relevant compounds (O_3 and $PM_{2.5}$) over West Africa during the DACCIWA period. We compare the model with the 'improved' DACCIWA and the GFAS emissions described in Section 6.2 and the equivalent simulation without the biomass burning emissions to evaluate the influence of humans on the the composition over West Africa. Figure 25 shows the mean surface ozone distribution in the full simulation and then the absolute and percentage decrease in that concentration if the biomass burning emissions are switched off.

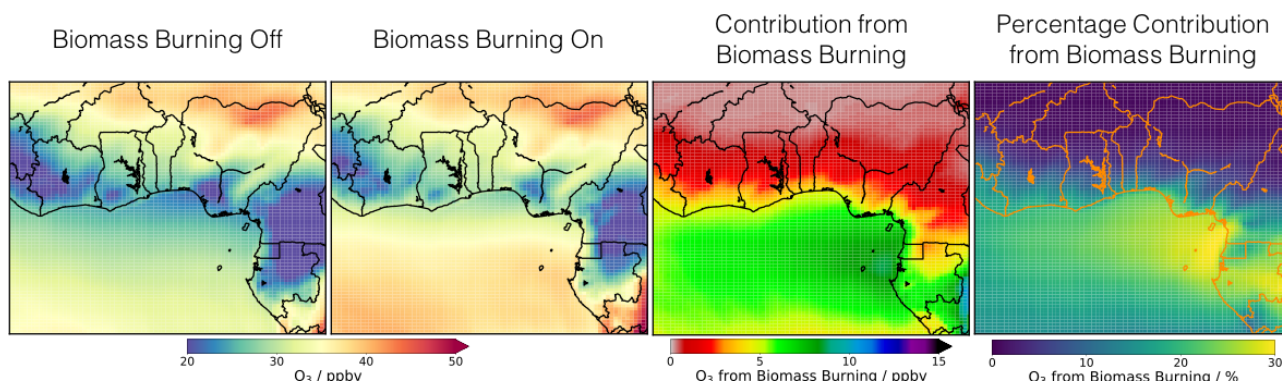


Figure 25. Surface mean ozone concentrations from the GEOS-Chem model (running from left to right) without biomass burning switched on, with biomass burning switched on, absolute difference and fractional difference.

Biomass burning increases the surface ozone by around 5 ppbv or 20% through the coastal region with this reducing northwards.

Figure 26 shows the mean PM_{2.5} concentration in the full simulation and then the percentage decrease in that concentration if the biomass burning emissions are switched off.

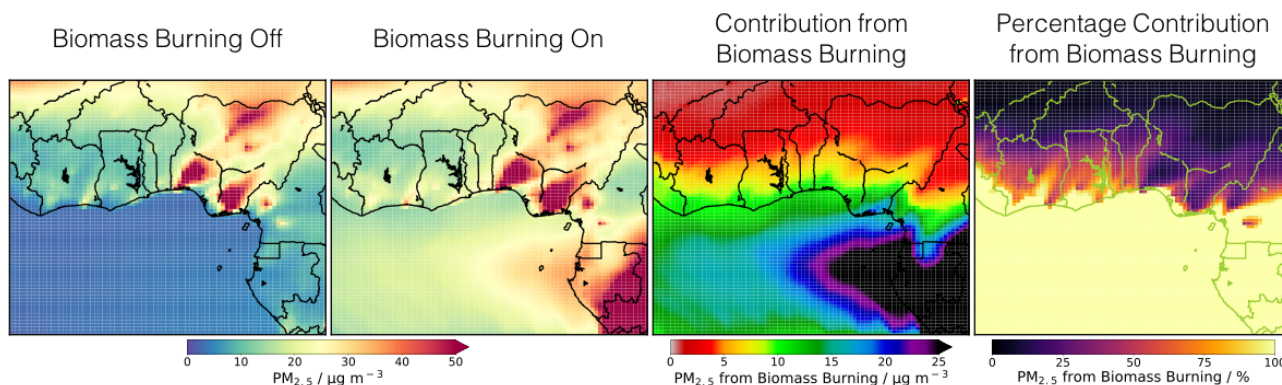


Figure 26. Surface mean PM_{2.5} concentrations from the GEOS-Chem model (running from left to right) without biomass burning switched on, with biomass burning switched on, absolute difference and fractional difference.

The impact of the biomass burning is more profound for PM_{2.5}. Here the simulation with the biomass burning switched off gives PM_{2.5} concentrations ~10 µg m⁻³ lower over the coastal strip. This is a significant concentration (equivalent to the WHO air quality standard) which would not be subject to local air quality management.

7.2 Impacts of anthropogenic emissions (UoY)

In this section we use the GEOS-Chem model to evaluate the impact of the anthropogenic emissions on policy relevant compounds (O₃ and PM_{2.5}) over West Africa during the DACCIWA period. We compare the model with the ‘improved’ DACCIWA emissions described in Section 6.2 and the equivalent simulation without the anthropogenic emissions to evaluate the influence of humans on the composition over West Africa.

Figure 27 shows the mean surface ozone distribution in the full simulation and then the percentage decrease in that concentration if the biomass burning emissions are switched off.

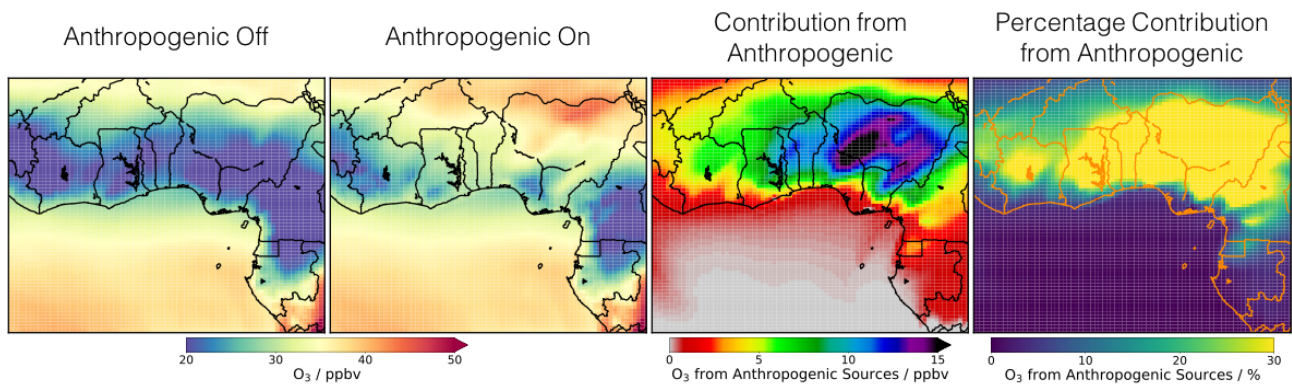


Figure 27. Surface mean ozone concentrations from the GEOS-Chem model (running from left to right) without anthropogenic emissions switched on, with anthropogenic emissions switched on, absolute difference and fractional difference.

Figure 28 shows the mean PM_{2.5} concentration in the full simulation and then the percentage decrease in that concentration if the anthropogenic emissions are switched off.

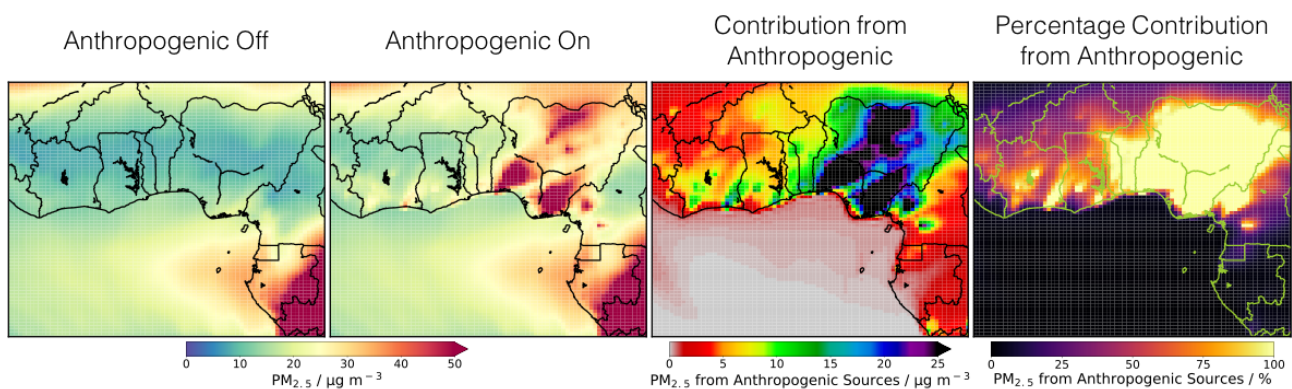


Figure 28. Surface mean PM_{2.5} concentrations from the GEOS-Chem model (running from left to right) without anthropogenic emissions switched on, with anthropogenic emissions switched on, absolute difference and fractional difference.

Anthropogenic emissions within the DACCIWA region create relatively small ozone production within the DACCIWA region. This averages around 10 ppbv or 30% (Figure 27). Much of this reflects the large natural emissions in the region. Organics are dominated by the natural isoprene source (Table 1) and NO_x emissions from soil are the largest individual source (Table 1). Thus anthropogenic emissions have a smaller impact on the O₃ concentration than might be anticipated. These concentrations are larger over inland Nigeria.

Anthropogenic emissions within the DACCIWA region have a larger impact on the PM_{2.5} concentrations. Over the cities, anthropogenic emissions make up a large fraction of the PM_{2.5} (Figure 28). Over Nigeria high concentrations of PM_{2.5} (>50 µg m⁻³) are entirely attributable to anthropogenic contributions.

8 DACCIWA Developed Emissions Inventories

8.1 Anthropogenic Emissions

An Africa-specific anthropogenic emission inventory has been developed by WP2 as part of the DACCIWA project (*deliverable 2.1; Junker et al. 2008*). This inventory contains emissions for CO, NO_x, SO₂, NMVOCs, OC and BC, based upon African emission factors, at a resolution of 0.125° x 0.125°. This inventory is available for the years 1990 to 2015. Emission of each of these species are provided for the following sectors: energy, flaring, industry, residential, traffic, waste and other. Figure 29 shows the total emissions of each of the species for the West Africa region.

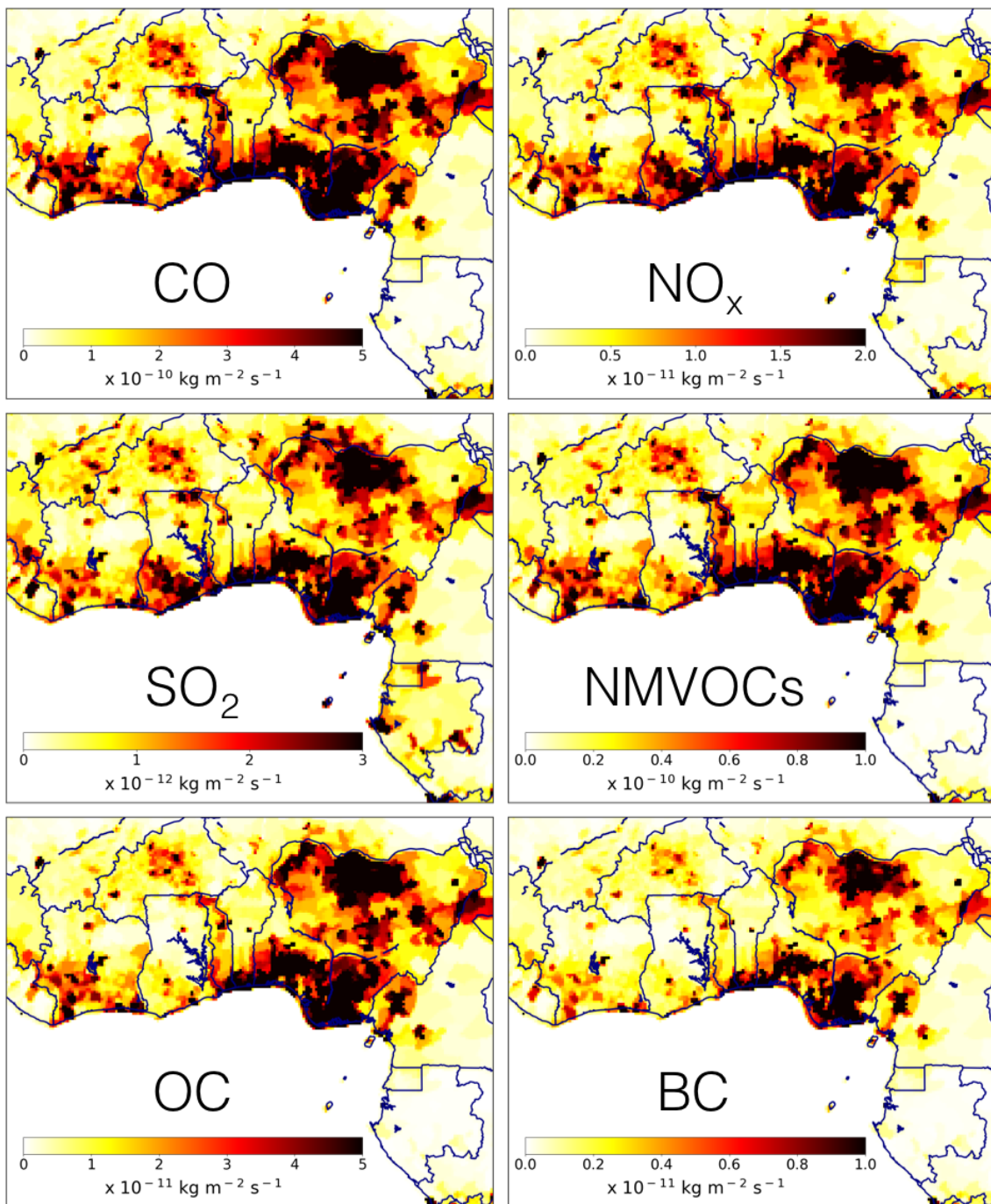


Figure 29: Emissions of CO, NO_x, SO₂, NMVOCs, OC, and BC from the DACCIWA anthropogenic inventory for the year 2015 for West Africa.

8.2 Oil Flaring

Deetz and Vogel [2017] developed an emissions inventory for gas flaring in the Gulf of Guinea as part of the DACCIWA project. Based on night time satellite observations of light coming from the region it developed emissions inventories for CO, CO₂, NO, NO₂ and SO₂.

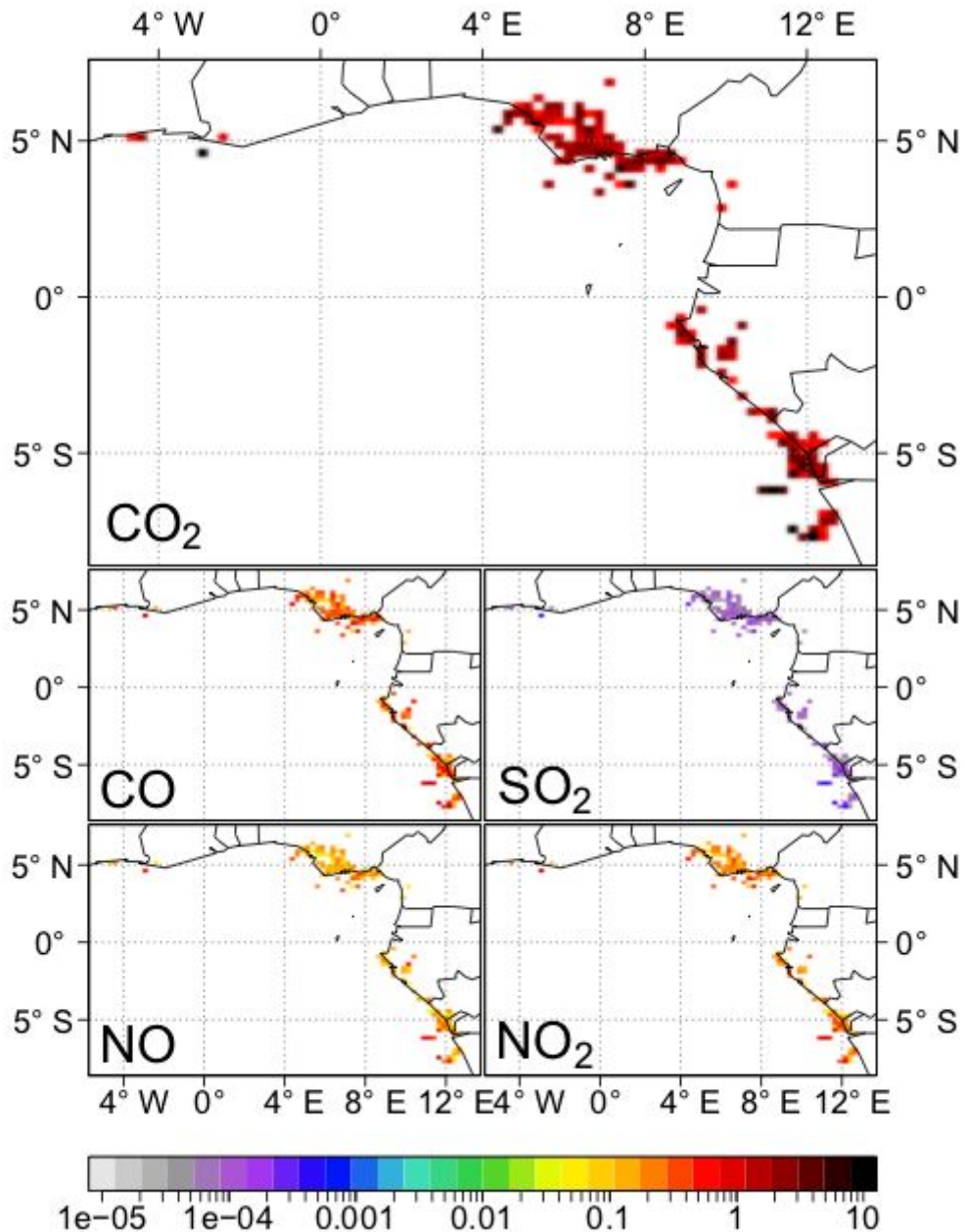


Figure 30. Gas flaring emission in the DACCIWA region from Deetz and Vogel [2017]

This showed that most of the flaring emissions were located in Nigeria and through into the coastal regions of central Africa. This is in general away from the region of most focus for DACCIWA.

9.0 Conclusions

This report highlights number of studies within the DACCIWA project that have been conducted to assess the quality of the emissions in the southern West African region. In general they show a significant underestimation in the magnitude of the anthropogenic emissions in the region compared to internationally recognized standards emissions. Emissions of CO, OC and BC appear to be consistent with current emissions. However emissions of NO_x, appear to need to be increased by factors of between 3 and 10 compared to the EDGAR emissions inventory and 50% from the DACCIWA emissions. SO₂ emissions need to be increased by a factor of 10. VOC emissions need to be increased by factors of 50. Uncertainties between the emissions are large but it appears highly likely that current estimates of the emissions from the region are significantly underestimated.

This uncertainty in the emissions have a profound impact on the air quality composition of the region especially for particulates. The difference in average PM over the southern West African cities calculated by a model with what are considered the standard international emissions (EDGAR) and those calculated by Africa specific DACCIWA emissions scaled to fit the observations is a factor of 4. Thus any model based assessment of the air quality in southern West Africa using the standard emissions will likely under-estimate policy relevant parameters such as O₃ and PM_{2.5}.

Bibliography

- Alexander, B., Park, R. J., Jacob, D. J., Li, Q. B., Yantosca, R. M., Savarino, J., ... Thiemens, M. H. (2005). Sulfate formation in sea-salt aerosols: Constraints from oxygen isotopes. *Journal of Geophysical Research*, 110(D10), D10307. <https://doi.org/10.1029/2004JD005659>
- Bey, I., Jacob, D. J., Yantosca, R. M., Logan, J. A., Field, B. D., Fiore, A. M., ... Schultz, M. G. (2001). Global modeling of tropospheric chemistry with assimilated meteorology: Model description and evaluation. *Journal of Geophysical Research*, 106095(16), 73–23. <https://doi.org/10.1029/2001JD000807>
- Breider, T. J., Mickley, L. J., Jacob, D. J., Ge, C., Wang, J., Payer Sulprizio, M., ... Hopke, P. K. (2017). Multidecadal trends in aerosol radiative forcing over the Arctic: Contribution of changes in anthropogenic aerosol to Arctic warming since 1980. *Journal of Geophysical Research: Atmospheres*, 122(6), 3573–3594. <https://doi.org/10.1002/2016JD025321>
- Brosse, F., Leriche, M., Mari, C., & Couvreur, F. (2018). LES study of the impact of moist thermals on the oxidative capacity of the atmosphere in southern West Africa. *Atmospheric Chemistry and Physics*, 18(9), 6601–6624. <https://doi.org/10.5194/acp-18-6601-2018>
- Deetz, K. and Vogel, B. (2017). Development of a new gas-flaring emission dataset for southern West Africa. *Geosci. Mod. Dev.*, 10, 1607–1620. [doi:10.5194/gmd-10-1607-2017](https://doi.org/10.5194/gmd-10-1607-2017)
- Djossou, J., Léon, J.-F., Akpo, A. B., Lioussé, C., Yoboué, V., Bedou, M., ... Awanou, C. N. (2018). Mass concentration, optical depth and carbon composition of particulate matter in the major southern West African cities of Cotonou (Benin) and Abidjan (Côte d'Ivoire). *Atmospheric Chemistry and Physics*, 18(9), 6275–6291. <https://doi.org/10.5194/acp-18-6275-2018>
- EC-JRC / PBL: Emission Database for Global Atmospheric Research (EDGAR), release version 4.2. European Commission, Joint Research Centre (JRC)/Netherlands Environmental Assessment Agency (PBL), <http://edgar.jrc.ec.europa.eu>, 2011.
- Flamant, C., Knippertz, P., Fink, A. H., Akpo, A., Brooks, B., Chiu, C. J., ... Yoboué, V. (2018). The Dynamics–Aerosol–Chemistry–Cloud Interactions in West Africa Field Campaign: Overview and Research Highlights. *Bulletin of the American Meteorological Society*, 99(1), 83–104. <https://doi.org/10.1175/BAMS-D-16-0256.1>
- Guenther, A. B., Jiang, X., Heald, C. L., Sakulyanontvittaya, T., Duhl, T., Emmons, L. K., & Wang, X. (2012). The Model of Emissions of Gases and Aerosols from Nature version 2.1 (MEGAN2.1): an extended and updated framework for modeling biogenic emissions. *Geoscientific Model Development*, 5(6), 1471–1492. <https://doi.org/10.5194/gmd-5-1471-2012>
- He, H., Wang, Y., Ma, Q., Ma, J., Chu, B., Ji, D., ... Hao, J. (2015). Mineral dust and NO_x promote the conversion of SO₂ to sulfate in heavy pollution days. *Scientific Reports*, 4(1), 4172. <https://doi.org/10.1038/srep04172>

- Heil, A., Kaiser, J. W., Van Der Werf, G. R., Wooster, M. J., & Schultz, M. G. (2010) Assessment of the Real-Time Fire Emissions (GFASv0) by MACC. Tech. Memo. 628, ECMWF, Reading, UK.
- Huang, G., Brook, R., Crippa, M., Janssens-Maenhout, G., Schieberle, C., Dore, C., ... Friedrich, R. (2017). Speciation of anthropogenic emissions of non-methane volatile organic compounds: a global gridded data set for 1970–2012. *Atmospheric Chemistry and Physics*, 17(12), 7683–7701. <https://doi.org/10.5194/acp-17-7683-2017>
- Hudman, R. C., Moore, N. E., Mebust, A. K., Martin, R. V., Russell, A. R., Valin, L. C., & Cohen, R. C. (2012). Steps towards a mechanistic model of global soil nitric oxide emissions: implementation and space based-constraints. *Atmospheric Chemistry and Physics*, 12(16), 7779–7795. <https://doi.org/10.5194/acp-12-7779-2012>
- Jaeglé, L., Quinn, P. K., Bates, T. S., Alexander, B., & Lin, J.-T. (2011). Global distribution of sea salt aerosols: new constraints from in situ and remote sensing observations. *Atmospheric Chemistry and Physics*, 11(7), 3137–3157. <https://doi.org/10.5194/acp-11-3137-2011>
- Janssens-Maenhout, G., Crippa, M., Guizzardi, D., Dentener, F., Muntean, M., Pouliot, G., ... Li, M. (2015). HTAP_v2.2: a mosaic of regional and global emission grid maps for 2008 and 2010 to study hemispheric transport of air pollution. *Atmospheric Chemistry and Physics*, 15(19), 11411–11432. <https://doi.org/10.5194/acp-15-11411-2015>
- Junker, C., & Liousse, C. (2008). A global emission inventory of carbonaceous aerosol from historic records of fossil fuel and biofuel consumption for the period 1860;1997. *Atmospheric Chemistry and Physics*, 8(5), 1195–1207. <https://doi.org/10.5194/acp-8-1195-2008>
- Kaiser, J. W., Flemming, J., Schultz, M. G., Suttie, M., Wooster, M. J. (2009) The MACC Global Fire Assimilation System: First Emission Products (GFASv0), Tech. Memo. 596, ECMWF, Reading, UK
- Kaiser, J. W., Heil, A., Andreae, M. O., Benedetti, A., Chubarova, N., Jones, L., ... van der Werf, G. R. (2012). Biomass burning emissions estimated with a global fire assimilation system based on observed fire radiative power. *Biogeosciences*, 9(1), 527–554. <https://doi.org/10.5194/bg-9-527-2012>
- Keita, S., Liousse, C., Yoboué, V., Dominutti, P., Guinot, B., Assamoi, E.-M., ... Roblou, L. (2017). Aerosol and VOC emission factor measurements for African anthropogenic sources. *Atmospheric Chemistry and Physics Discussions*, 1–40. <https://doi.org/10.5194/acp-2017-944>. Accepted for final publication
- Knippertz, P., Fink, A. H., Deroubaix, A., Morris, E., Tocquer, F., Evans, M. J., ... Schlueter, A. (2017). A meteorological and chemical overview of the DACCIWA field campaign in West Africa in June–July 2016. *Atmospheric Chemistry and Physics*, 17(17), 10893–10918. <https://doi.org/10.5194/acp-17-10893-2017>
- Lamarque, J.-F., Bond, T. C., Eyring, V., Granier, C., Heil, A., Klimont, Z., ... van Vuuren, D. P. (2010). Historical (1850–2000) gridded anthropogenic and biomass burning emissions

- of reactive gases and aerosols: methodology and application. *Atmospheric Chemistry and Physics*, 10(15), 7017–7039. <https://doi.org/10.5194/acp-10-7017-2010>
- Lohmann, U., & Roeckner, E. (1996). Design and performance of a new cloud microphysics scheme developed for the ECHAM general circulation model. *Climate Dynamics*, 12(8), 557–572. <https://doi.org/10.1007/BF00207939>
- Lohmann, U., Stier, P., Hoose, C., Ferrachat, S., Kloster, S., Roeckner, E., & Zhang, J. (2007). Cloud microphysics and aerosol indirect effects in the global climate model ECHAM5-HAM. *Atmospheric Chemistry and Physics*, 7(13), 3425–3446. <https://doi.org/10.5194/acp-7-3425-2007>
- Mailler, S., Menut, L., Khvorostyanov, D., Valari, M., Couvidat, F., Siour, G., ... Meleux, F. (2017). CHIMERE-2017: from urban to hemispheric chemistry-transport modeling. *Geoscientific Model Development*, 10(6), 2397–2423. <https://doi.org/10.5194/gmd-10-2397-2017>
- Menut, L., Bessagnet, B., Khvorostyanov, D., Beekmann, M., Blond, N., Colette, A., ... Vivanco, M. G. (2013). CHIMERE 2013: a model for regional atmospheric composition modelling. *Geoscientific Model Development*, 6(4), 981–1028. <https://doi.org/10.5194/gmd-6-981-2013>
- Menut, L., Flamant, C., Turquety, S., Deroubaix, A., Chazette, P., & Meynadier, R. (2018). Impact of biomass burning on pollutant surface concentrations in megacities of the Gulf of Guinea. *Atmospheric Chemistry and Physics*, 18(4), 2687–2707. <https://doi.org/10.5194/acp-18-2687-2018>
- Murray, L. T., Jacob, D. J., Logan, J. A., Hudman, R. C., & Koshak, W. J. (2012). Optimized regional and interannual variability of lightning in a global chemical transport model constrained by LIS/OTD satellite data. *Journal of Geophysical Research: Atmospheres*, 117(D20). <https://doi.org/10.1029/2012JD017934>
- Pacifico, F., Delon, C., Jambert, C., Durand, P., Morris, E., Evans, M. J., ... Brilouet, P.-E. (2018). Measurements of nitric oxide and ammonia soil fluxes from a wet savanna ecosystem site in West Africa during the DACCIWA field campaign. *Atmospheric Chemistry and Physics Discussions*, 1–37. <https://doi.org/10.5194/acp-2017-1198>
- Roeckner, E., Bäuml, G., Bonaventura, L., Brokopf, R., Esch, M., Giorgetta, M., ... Tompkins, A. (2003) The atmospheric general circulation model ECHAM5. Part I: Model description. Report 349, Max Planck Institute for Meteorology, Hamburg, Germany.
- Sherwen, T., Evans, M. J., Carpenter, L. J., Schmidt, J. A., & Mickley, L. J. (2017). Halogen chemistry reduces tropospheric O₃ radiative forcing. *Atmos. Chem. Phys*, 17, 1557–1569. <https://doi.org/10.5194/acp-17-1557-2017>
- Stevens, B., Giorgetta, M., Esch, M., Mauritsen, T., Crueger, T., Rast, S., ... Roeckner, E. (2013). Atmospheric component of the MPI-M Earth System Model: ECHAM6. *Journal of Advances in Modeling Earth Systems*, 5(2), 146–172. <https://doi.org/10.1002/jame.20015>

- Stier, P., Feichter, J., Kinne, S., Kloster, S., Vignati, E., Wilson, J., ... Petzold, A. (2005). The aerosol-climate model ECHAM5-HAM. *Atmospheric Chemistry and Physics*, 5(4), 1125–1156. <https://doi.org/10.5194/acp-5-1125-2005>
- Turquety, S., Menut, L., Bessagnet, B., Anav, A., Viovy, N., Maignan, F., & Wooster, M. (2014). APIFLAME v1.0: high-resolution fire emission model and application to the Euro-Mediterranean region. *Geoscientific Model Development*, 7(2), 587–612. <https://doi.org/10.5194/gmd-7-587-2014>
- Vignati, E., Wilson, J., & Stier, P. (2004). M7: An efficient size-resolved aerosol microphysics module for large-scale aerosol transport models. *Journal of Geophysical Research: Atmospheres*, 109(D22), n/a-n/a. <https://doi.org/10.1029/2003JD004485>
- Zender, C. S., Bian, H., & Newman, D. (2003a). Mineral Dust Entrainment and Deposition (DEAD) model: Description and 1990s dust climatology. *Journal of Geophysical Research*, 108(D14), 4416. <https://doi.org/10.1029/2002JD002775>
- Zender, C. S., Newman, D., & Torres, O. (2003b). Spatial heterogeneity in aeolian erodibility: Uniform, topographic, geomorphic, and hydrologic hypotheses. *Journal of Geophysical Research*, 108(D17), 4543. <https://doi.org/10.1029/2002JD003039>
- Zhang, K., O'Donnell, D., Kazil, J., Stier, P., Kinne, S., Lohmann, U., ... Feichter, J. (2012). The global aerosol-climate model ECHAM-HAM, version 2: sensitivity to improvements in process representations. *Atmospheric Chemistry and Physics*, 12(19), 8911–8949. <https://doi.org/10.5194/acp-12-8911-2012>